UC-34a
LBL-17488
Preprint c.1

Lawrence Berkeley Laboratory
UNIVERSITY OF CALIFORNIA

Materials & Molecular Research Division

RECEIVED
LAWRENCE
BERKELEY LABORATORY
JUL 24 1984
LIBRARY AND
DOCUMENTS SECTION

Submitted to Physical Review B

GENERATION OF NONEQUILIBRIUM OPTICAL PHONONS IN GaAs AND THEIR APPLICATION IN STUDYING INTERVALLEY ELECTRON-PHONON SCATTERING

C.L. Collins and P.Y. Yu

For Reference
Not to be taken from this room

June 1984

Prepared for the U.S. Department of Energy under Contract DE-AC03-76SF00098

LBL-17488 c.1

DISCLAIMER

This document was prepared as an account of work sponsored by the United States Government. While this document is believed to contain correct information, neither the United States Government nor any agency thereof, nor the Regents of the University of California, nor any of their employees, makes any warranty, express or implied, or assumes any legal responsibility for the accuracy, completeness, or usefulness of any information, apparatus, product, or process disclosed, or represents that its use would not infringe privately owned rights. Reference herein to any specific commercial product, process, or service by its trade name, trademark, manufacturer, or otherwise, does not necessarily constitute or imply its endorsement, recommendation, or favoring by the United States Government or any agency thereof, or the Regents of the University of California. The views and opinions of authors expressed herein do not necessarily state or reflect those of the United States Government or any agency thereof or the Regents of the University of California.

Submitted to Physical Review B

Generation of Nonequilibrium Optical Phonons in GaAs and Their Application in Studying Intervalley Electron-Phonon Scattering

C. L. Collins and P. Y. Yu

Department of Physics, University of California, Berkeley, California 94720 and Materials and Molecular Research Division, Lawrence Berkeley Laboratory, Berkeley, Calfiornia 94720

Abstract

We present a detailed theoretical and experimental investigation of the generation and detection of nonequilibrium longitudinal optical (LO) phonons in GaAs by picosecond laser pulses. The nonequilibrium LO phonons are excited by the relaxation of energetic electron and hole pairs created by a tunable and modelocked dye laser. The photoexcited LO phonon population, monitored by Raman scattering with the same excitation laser pulses, is measured as a function of the excitation photon energy keeping the laser power constant. The phonon population was found to increase monotonically with photon energy between 1.75 and 1.95 eV. Above 1.95 eV the phonon population became roughly constant until at 2.105eV the phonon population suddenly decreased by approximately a factor of two. The experimental results are compared with several theoretical model calculations. We found that a simple parabolic bands model failed to explain the experimental results. Only by using a realistic band structure for GaAs did we achieve quantitative agreement between theory and experiment. In particular the experimental results turned out to be very sensitive to details of the band structure of GaAs such as nonparabolicity of the Γ_1 conduction band, warping of the

valence bands and presence of higher conduction band minima at zone boundaries. Specifically the sudden decrease in the LO phonon population at 2.105 eV is attributed to transfer of energetic electrons from the Γ_1 valley to the higher energy minima near the X points. By analyzing this decrease we were able to determine precisely the values of intervalley electron-phonon deformation potentials.

I. INTRODUCTION

It has been known for some time that energetic carriers in polar semiconductors, such as GaAs, are scattered very strongly by the longitudinal optical (LO) phonons via the Fröhlich interaction.[1] For example theoretical calculations of Conwell and Vassel[2] have predicted electron-LO phonon scattering rates of $>10^{12}\text{sec}^{-1}$ in GaAs. Thus for carriers in GaAs with kinetic energy E much larger than the LO phonon energy ($\hbar\omega_{LO}$) the predominant relaxation mechanism is by emission of LO phonons. The validity of this picture in many polar semiconductors has been verified directly by experiments such as oscillatory photoconductivity[3] and oscillatory photoluminescence spectroscopy.[4] More recently it has been realized by many authors that this relaxation mechanism can become an efficient way to generate a high transient population of non-thermal equilibrium LO phonons. Shah et al.[5] used a continuous wave Ar^+ laser to create the nonequilibrium LO phonons in GaAs and to probe this population by Raman scattering. They determined the lattice temperature of the sample to be ~400 K while the observed LO phonon population corresponded to a temperature of ~800 K. As a result they labelled these nonequilibrium phonons as hot phonons, although they have not determined whether these optical phonons are in equilibrium among themselves or not. Subsequently Mattos and Leite[6] showed that nonequilibrium optical phonons can be generated with the same technique in other semiconductors besides GaAs. Von der Linde et al.[7] utilized picosecond (psec) dye laser pulses to generate nonequilibrium LO phonons in GaAs and measured the time dependence of the LO phonon population by Raman scattering with a delayed picosecond probe pulse. They found the lifetime of the LO phonon

population to be ~7 psec at 77 K. Finally, Tsen et al.[8] recently showed that nonequilibrium acoustic phonons can also be excited by intense laser pulses in GaAs.

These earlier works have shown quite conclusively the feasibility of generating nonequilibrium phonons by optical pumping. Although the experimental results can be qualitatively understood based on existing theories, there are few quantitative theories predicting the nonequilibrium phonon population for comparison with experiment.[9] Also the experimental results have been obtained at only one or two discrete laser frequencies. Because of the uncertainty in the photoexcited carrier densities, the measured phonon populations are not critical tests of the theories.

In this paper we present a detailed experimental and theoretical investigation of the optical generation of nonequilibrium LO phonons in GaAs.[10] We used a modelocked dye laser as the source of tunable picosecond pulses for exciting the nonequilibrium LO phonons. The tunability of the laser enabled us to measure the phonon population as a function of the photon energy and hence the carrier energy. This photon energy dependence of the phonon population turned out to be a very sensitive test of any theoretical model of the phonon generation process. We found good agreement between experiment and theory only if we assumed a realistic band structure for GaAs. In particular, when the photoexcited electron energy is high enough to scatter into the higher energy conduction band minima at the X points of the Brillouin zone,[11] this intervalley electron-phonon scattering has a pronounced effect on the nonequilibrium LO phonon population. We showed that, because of the

competition between intervalley and intravalley electron-phonon scattering mechanisms, nonequilibrium phonon populations can be utilized to determine the deformation potentials of intervalley electron-phonon interactions.

The organization of this paper is as follows. Section II presents the theory of optical generation of nonequilibrium phonons based on various models of the band structure of the semiconductor. Section III presents the experimental setup we used to measure the nonequilibrium phonon population and the results we obtained. In Section IV we compare the experimental results with the theoretical curves based on the different band models. The discussions and conclusions are summarized in Section V.

II. Theoretical Models for Calculation of Nonequilibrium LO Phonons in GaAs

The problem we are trying to address in this paper has many overlaps with the phenomena of hot electrons and stimulated Raman scattering. Many excellent review articles already exist on these topics so we will not elaborate on them other than to point out their connection to the present work.

We will consider in this paper the generation of phonons due to relaxation of hot carriers in GaAs. The transport properties of such hot carriers when excited by high electric field have been investigated for many years. In particular in GaAs it is well-known that the transfer of hot electrons from the central Γ minimum to the higher energy X minima is responsible for the Gunn effect.[1] In connection with these

efforts, the electron-phonon scattering rates in GaAs have been calculated in great detail by Conwell and coworkers.[1,2] On the other hand, non-equilibrium phonons have also been generated by stimulated Raman and Brillouin scatterings in many media.[12] These studies have provided important information on the dephasing and decaying mechanisms of phonons. The present work differs from these experiments in that we generate an incoherent population of phonons via relaxation of hot carriers whereas in stimulated scattering a phonon population coherent with the incident radiation is excited via Raman scattering. In both cases optically excited phonon population is probed by Raman scattering.

To our knowledge the first theoretical attempt to calculate optically generated LO phonon population in GaAs was reported by Levinson and Levinsky.[9] This paper forms the starting point of our calculation but differs from our work in the following respects. (1) We have performed a time-dependent calculation because of the picosecond duration of our pulses. (2) We have solved the rate equations for the electron and phonon populations numerically. (3) We have used a realistic band structure of GaAs including the nonparabolicity of the conduction band, the warping of the valence bands and the presence of higher conduction band minima at the X and L points of the Brillouin zone.

A. Qualitative Description of Model

Since our calculation utilizing the actual band structure of GaAs is rather involved, we will first present a qualitative description of our model and outline the essential ideas and assumptions behind our calculation.

Let us assume that the band structure of GaAs can be approximated by two parabolic bands separated by an energy gap E_g of 1.52 eV. A nearly monochromatic laser pulse of photon energy $\hbar\omega_i$ is used to excite electrons from the filled valence band (VB) to the empty conduction band (CB) as shown by the vertical arrow in Fig. 1. The energy distributions of the excited electrons and holes will be monoenergetic if carrier-carrier collision is negligible. This has been shown to be the case if the photoexcited carrier densities are $<<10^{17}cm^{-3}$ [1,2] which is satisfied in our experiment. In GaAs it is known that the excited electrons and holes will relax towards their respective band extrema by a cascade of LO phonon emission. The time to emit a LO phonon τ_{e-LO} has been estimated to be ~0.1 psec.

Since the LO phonon energy ($\hbar\omega_{LO}$) in GaAs is equal to 0.037 eV, even electrons with kinetic energy of the order of 0.5 eV will take only about 1 psec to relax to the band minima. On the other hand the LO phonons emitted in the cascade process have lifetimes of ~7 psec.[7] Thus a transient nonequilibrium LO phonon population can be generated by a laser pulse of picosecond duration and with $\hbar\omega_i >> E_g$. Furthermore, this LO phonon population should increase with increase in $\hbar\omega_i$.

The above picture is valid provided the energetic carriers relax predominantly by LO phonon emission. This is true in GaAs when the electrons are not energetic enough to scatter into higher conduction band minima at the L and X points of the Brillouin zone.[13] These inter-valley scatterings can occur when the electron energy E is larger than ~0.3 eV and ~0.5 eV respectively. In particular the scattering time to the X valleys is known to be much shorter than τ_{e-LO} in order to explain

the Gunn effect in GaAs. Thus we expect a drop in the photoexcited LO phonon population when $\hbar\omega_i$ is large enough so that the electrons can scatter into the X valleys.

To make this model accurate enough for quantitative comparisons with experimental results, we have to consider complications due to deviations of the band structure of GaAs from the simple two parabolic bands model. These band structure effects include the nonparabolicity of the conduction band and the warping of the valence bands. Another effect which has not been considered by other authors relates to the fact that Raman scattering is utilized to measure the phonon population. While the relaxation of hot carriers typically generates LO phonons with a range of wavevectors, Raman scattering can probe only LO phonon with rather small wavevectors. As a result we found that the number of nonequilibrium LO phonons observed in Raman scattering saturates as the photon energy becomes larger than ~2.0 eV.

B. Two Parabolic Bands Model

We will first carry out the calculation for the simple two parabolic bands model shown in Fig. 1. For simplicity we will assume that the excited carriers interact with LO phonons only and that dispersion of the LO phonon in GaAs is negligible. Although both electrons and holes are excited we will assume that the electron mass (m*) is much smaller than the hole mass so that most of the excess energy $\hbar\omega_i - E_g$ of the photon goes to the electron.[14] For simplicity we will neglect the phonons emitted by the relaxation of the holes. With these assumptions we have only two populations to consider: $f_{\bar{K}}(t)$, the occupation number of electrons with wavevector $\bar{K}$ and $N_{\bar{q}}(t)$, the occupation number

of LO phonons with wavevector $\bar{q}$. The two distributions can be calculated as a function of time by solving two Boltzmann equations:

$$\frac{df_{\bar{K}}}{dt} = G_{\bar{K}} + \left(\frac{\partial f_{\bar{K}}}{\partial t}\right)_{LO} - \frac{f_{\bar{K}}}{\tau_{\bar{K}}} \tag{1}$$

$$\frac{dN_{\bar{q}}}{dt} = \left(\frac{\partial N_{\bar{q}}}{\partial t}\right)_{e} - \frac{N_{\bar{q}}}{\tau_{LO}} \tag{2}$$

In Eq. (1) $G_{\bar{K}}$ is the rate of generation of electrons due to optical excitation, $\left(\frac{\partial f_{\bar{K}}}{\partial t}\right)_{LO}$ is the rate of change in electron occupation number due to scattering with LO phonons, and $\tau_{\bar{K}}$ is the electron lifetime due to any other decaying processes, such as radiative and non-radiative recombinations. In Eq.(2) $\left(\frac{\partial N_{\bar{q}}}{\partial t}\right)_{e}$ is the rate of change in the LO phonon occupation number due to its interaction with the electrons while τ_{LO} is the lifetime of LO phonons due to their decay into acoustic phonons. For simplicity τ_{LO} is assumed to be independent of $\bar{q}$ and has the value of 7 ps in GaAs as determined by von der Linde et al.[7]

The rates $\left(\frac{\partial f_{\bar{K}}}{\partial t}\right)_{LO}$ and $\left(\frac{\partial N_{\bar{q}}}{\partial t}\right)_{e}$ can be calculated from time-dependent perturbation theory. It has been shown that the electron-LO phonon interaction in GaAs is dominated by the Fröhlich interaction, H'. We will represent the matrix element of H' for scattering an electron in state $\bar{K}$ to $\bar{K}-\bar{q}$ (or $\bar{K}+\bar{q}$) with emission (or absorption) of an LO phonon with wave vector $\bar{q}$ as $M_{\bar{K},\bar{K}\pm\bar{q}} = |\langle \bar{K}|H'|\bar{K}\pm\bar{q}\rangle|^2$. Using Fermi's Golden Rule we can write $\left(\frac{\partial f_{\bar{K}}}{\partial t}\right)_{LO}$ as:

$$\left(\frac{\partial f_{\bar{K}}}{\partial t}\right)_{LO} = \frac{2\pi}{\hbar} \sum_{\bar{q}} \Big[- M_{\bar{K},\bar{K}-\bar{q}}(N_{\bar{q}} + 1) f_{\bar{K}}(1 - f_{\bar{K}-\bar{q}}) \delta(E_{\bar{K}} - E_{\bar{K}-\bar{q}} - \hbar\omega_{LO})$$
$$- M_{\bar{K},\bar{K}+\bar{q}} N_{\bar{q}} f_{\bar{K}}(1 - f_{\bar{K}+\bar{q}}) \delta(E_{\bar{K}} - E_{\bar{K}+\bar{q}} + \hbar\omega_{LO})$$
$$+ M_{\bar{K}+\bar{q},\bar{K}}(N_{\bar{q}} + 1)(1 - f_{\bar{K}}) f_{\bar{K}+\bar{q}} \delta(E_{\bar{K}+\bar{q}} - E_{\bar{K}} - \hbar\omega_{LO})$$
$$+ M_{\bar{K}-\bar{q},\bar{K}} N_{\bar{q}}(1 - f_{\bar{K}}) f_{\bar{K}-\bar{q}} \delta(E_{\bar{K}-\bar{q}} - E_{\bar{K}} + \hbar\omega_{LO}) \Big] \tag{3}$$

The first two terms in Fig. (3) arise from the decay of the electron in state $\bar{K}$ with emission or absorption of a LO phonon. The last two terms are due to scattering of electrons in other states into the state $\bar{K}$ via emission or absorption of a LO phonon. Since these scattering processes also generate the LO phonons we find that

$$\left(\frac{\partial N_{\bar{q}}}{\partial t}\right)_e = \frac{2\pi}{\hbar} \sum_{\bar{K}} \Big[M_{\bar{K},\bar{K}-\bar{q}}(N_{\bar{q}} + 1) f_{\bar{K}}(1 - f_{\bar{K}-\bar{q}}) \times$$
$$\delta(E_{\bar{K}} - E_{\bar{K}-\bar{q}} - \hbar\omega_{LO}) -$$
$$M_{\bar{K},\bar{K}+\bar{q}} N_{\bar{q}} f_{\bar{K}} (1 - f_{\bar{K}+\bar{q}}) \delta(E_{\bar{K}} - E_{\bar{K}+\bar{q}} + \hbar\omega_{LO}) \Big] \tag{4}$$

$E_{\bar{K}}$ in Eqs. (3) and (4) is the energy of the electron in state $\bar{K}$. If we assume the conduction band of GaAs to be spherical with Γ_1(s-like) symmetry and effective mass m* then[1]

$$E_{\bar{K}} = \frac{\hbar^2 K^2}{2m^*} \tag{5}$$

and

$$M_{\bar{K},\bar{K}+\bar{q}} = \frac{2\pi\hbar^2 e \mathcal{E}_o}{V m^* q^2} \tag{6}$$

where e is the electronic charge, V is the volume of crystal and $\mathcal{E}_o$ is the longitudinal electric field associated with the LO phonon. $\mathcal{E}_o$ is given by[1]

$$\mathcal{E}_o = \frac{m^* e \omega_{LO}}{\hbar} \left(\frac{1}{\varepsilon_\infty} - \frac{1}{\varepsilon_o} \right) \tag{7}$$

where ε_∞ and ε_o respectively are the high frequency and low frequency dielectric constants of the material. By assuming that the electron distribution is nondegenerate ($f_K \ll 1$), substituting Eqs. (5) and (6) into Eqs. (4) and (3) and integrating over the delta functions, we obtain

$$\left(\frac{\partial N_q}{\partial t} \right)_e = \frac{2m^* e \mathcal{E}_o}{\hbar^3 q^3} \left[\int_{E_{max}}^{\infty} f_K \, dE_K - N_q \int_{E_{min}}^{E_{max}} f_K \, dE_K \right] \tag{8}$$

and

$$\left(\frac{\partial f(E,t)}{\partial t} \right)_{LO} = \frac{e \mathcal{E}_o}{\sqrt{2m^* E}} \left\{ \left(f(E_+) - f(E) \right) \int_{\frac{\sqrt{2m^*}}{\hbar}(\sqrt{E_+} - \sqrt{E})}^{\frac{\sqrt{2m^*}}{\hbar}(\sqrt{E} + \sqrt{E_+})} \frac{N_q \, dq}{q} + \right.$$

$$\left(f(E_-) - f(E) \right) \int_{\frac{\sqrt{2m^*}}{\hbar}(\sqrt{E} - \sqrt{E_-})}^{\frac{\sqrt{2m^*}}{\hbar}(\sqrt{E} + \sqrt{E_-})} \frac{N_q \, dq}{q} +$$

$$\left. f(E_+) \, \ln \left(\frac{\sqrt{E_+} + \sqrt{E}}{\sqrt{E_+} - \sqrt{E}} \right) - f(E) \, \ln \left(\frac{\sqrt{E} + \sqrt{E_-}}{\sqrt{E} - \sqrt{E_-}} \right) \right\} \tag{9}$$

where $E_{max} = \frac{(E_q + \hbar\omega_{LO})}{4E_q}$, $E_{min} = \frac{(E_q - \hbar\omega_{LO})}{4E_q}$, $E_q = \frac{\hbar^2 q^2}{2m^*}$,

$$E_+ = E + \hbar\omega_{LO} \quad \text{and} \quad E_- = E - \hbar\omega_{LO} .$$

As shown by Levinson and Levinsky[9], if $\left(\frac{\partial f}{\partial E} \right) \hbar\omega_{LO} \ll f(E)$ then stimulated emission and absorption of phonons nearly cancel each other. Within this approximation Eqs. (1) and (2) are decoupled into:

$$\frac{df(E,t)}{dt} = \frac{e\mathcal{E}_o}{\sqrt{2m^*E}} \left\{ f(E_+t)\ln\left(\frac{\sqrt{E_+} + \sqrt{E}}{\sqrt{E_+} - \sqrt{E}}\right) - f(E,t)\ln\left(\frac{\sqrt{E} + \sqrt{E_-}}{\sqrt{E} - \sqrt{E_-}}\right)\right\} + G(E,t) - \frac{f}{\tau(E)} \tag{10}$$

and

$$\frac{dN_q}{dt} = -\frac{N_q}{\tau_{LO}} + \frac{2m^*e\mathcal{E}_o}{\hbar^3 q^3} \int_{E_{max}}^{\infty} f(E,t)dE \tag{11}$$

If we assume that the excitation pulse is a delta function in time and energy and $\tau(E)$ is infinite, Eq. (10) and (11) can be solved analytically. Both $f(E,t)$ and $N_q(t)$ can be expressed as a sum of exponential functions in time. The calculation is rather straightforward although lengthy so we will present it in Appendix I. Based on the solutions of Eq. (11) we have calculated the nonequilibrium LO phonon occupation number N_{LO} observed in Raman scattering as a function of excitation photon energy. For any given photon energy $\hbar\omega_i$, we set $E = \hbar\omega_i - E_g$ and compute $N_q(\hbar\omega_i)$ from Eq. (11). Next the wavevector of LO phonon observed in backward Raman scattering is calculated from the known refractive index $n(\omega)$ of GaAs: $q(\omega_i) \simeq \frac{2\omega_i n(\omega_i)}{c}$. An example of N_q for $\hbar\omega_i = 1.77$ eV is shown in Fig. 2 where $q(\omega_i)$ correspond to the hatched area. It turns out that for $\omega_i \lesssim 2.0$ eV the Raman wavevectors $q(\omega_i)$ coincide more or less with the peak in $N_q(\hbar\omega_i)$. For $\hbar\omega_i \gtrsim 2.0$ eV this is no longer the case for the peak in $N_q(\hbar\omega_i)$ tends to occur at values larger than $q(\omega_i)$. This leads to a saturation in the value of N_{LO} for $\hbar\omega_i \gtrsim 2.0$ eV as shown in Fig. 3. For comparison we have also included in Fig. 3 the results we would have obtained if we neglect the variation in q with $\hbar\omega_i$ and instead assume a constant q of $7\times10^5 cm^{-1}$. Notice how the inclusion of

the variation of q with $\hbar\omega_i$ smoothes the sharp steps in N_{LO} which are predicted by the simple model.

C. Parabolic Band Model Including Intervalley Scattering

Next we modify the above model by assuming a schematic band structure as shown in Fig. 4. This model is motivated by the well-known Gunn effect which results from the rapid transfer of hot electrons from the Γ valley to the X valleys.[13] Since it is known that the rate of Γ to X intervalley scattering in GaAs is even faster than the intravalley LO phonon emission rate[2] we cannot assume the electron lifetime τ(E) to be infinite. Instead τ(E) will be energy dependent as given by:

$$\tau(E) \simeq \begin{cases} \infty & E < E_{\Gamma L} \\ \gamma_{\Gamma L}^{-1} & E_{\Gamma L} < E < E_{\Gamma X} \\ (\gamma_{\Gamma L} + \gamma_{\Gamma X})^{-1} & E > E_{\Gamma X} \end{cases} \tag{12}$$

where $E_{\Gamma L}$ and $E_{\Gamma X}$ are the separations between the conduction band minimum at Γ and the mimima at L and X respectively. $\gamma_{\Gamma L}$ and $\gamma_{\Gamma X}$ represent the intervalley scattering rates from the Γ valley to the L and X valleys respectively.

Besides affecting the electron lifetime in the Γ valley, intervalley scattering causes the population of the Γ valley to become coupled to the population in the X and L valleys. As a result we have to introduce two additional equations for the populations in these valleys: f^X and f^L. For convenience f^X will represent the total population in all the X valleys and f^L represents the population in all the L valleys. Although these valleys are highly anisotropic we will assume that scatterings among the X valleys and among the L valleys occur almost

instantaneously so that the population in the degenerate valleys are equalized immediately.

To simplify the calculation, let us consider the following selection rules for intervalley electron-phonon scattering.[15]

Intervalley Scattering	Phonons Allowed by Selection Rules
$\Gamma \leftrightarrow X$	LO(X)
$\Gamma \leftrightarrow L$	LO(L) and LA(L)
$X \leftrightarrow L$	LO(L), TO(L), TA(L) and LA(L)

The zone edge phonon energies in GaAs plus other relevant parameters of GaAs are summarized in Table I. All the zone edge phonons except for TA(L) can be approximated as having a single frequency ω_{ZB} with $\hbar\omega_{ZB} \simeq$ 29.6 meV. There is evidence that the TA phonons are less effective in coupling the X and L valleys than the higher energy phonons so we will neglect its contribution to the intervalley scattering.[1] With this approximation we can essentially assume that a single phonon with energy $\hbar\omega_{ZB}$ is responsible for the intervalley scatterings. With these approximations the intervalley scattering rate $\gamma_{\Gamma X}$ can be calculated with the expression:[1]

$$\gamma_{\Gamma X} f(E) \cong \frac{D_{\Gamma X}^2 \sqrt{m_x^X m_y^X m_z^X}}{\sqrt{2}\pi\hbar^3 \rho \omega_{ZB}} \Big\{ (E + \hbar\omega_{ZB} - E_{\Gamma X})^{\frac{1}{2}} \Big[(N_{ZB} + 1) \times f^X(E + \hbar\omega_{ZB}) - 3N_{ZB} f(E) \Big] + (E - \hbar\omega_{ZB} - E_{\Gamma X})^{\frac{1}{2}} \times \Big[N_{ZB} f^X(E - \hbar\omega_{ZB}) - 3(N_{ZB} + 1) f(E) \Big] \Big\} \tag{13}$$

where ρ is the density, $D_{\Gamma X}$ is the deformation potential for the Γ to X intervalley electron-phonon interaction, m_x^X, m_y^X and m_z^X are the components

of the X valley effective mass tensor and N_{ZB} is the occupation number of the zone-edge optical phonons. We have no information as to whether these zone edge phonons are in thermal equilibrium or not. One may argue that they may not be in equilibrium because of bottleneck effects.[8] However, in the absence of any evidence to the contrary in our spectra, we will assume N_{ZB} to be given by the equilibrium value. As a consequence the terms proportional to N_{ZB} in Eq.(13) can all be neglected. The factor 3 in Eq.(13) takes care of the degeneracy of the X valleys. For $E>E_{\Gamma X}$ we obtain, under the above approximations, the intervalley scattering contribution to Eq.(10) as:

$$\begin{aligned}\left(\frac{\partial f}{\partial t}\right)_{\text{intervalley scattering}} &= (\gamma_{\Gamma X}+\gamma_{\Gamma L})f(E) \\ &\simeq \frac{D^2_{\Gamma X}\sqrt{m^X_x m^X_y m^X_z}}{\sqrt{2}\pi\hbar^3\rho\omega_{ZB}}\Big\{(E+\hbar\omega_{ZB}-E_{\Gamma X})^{\frac{1}{2}}f^X(E+\hbar\omega_{ZB}) - \\ &\quad 3(E-\hbar\omega_{ZB}-E_{\Gamma X})^{\frac{1}{2}}f(E)\Big\} + \\ &\quad \frac{D^2_{\Gamma L}\sqrt{m^L_x m^L_y m^L_z}}{\sqrt{2}\pi\hbar^3\rho\omega_{ZB}}\Big\{(E+\hbar\omega_{ZB}-E_{\Gamma L})^{\frac{1}{2}}f^L(E+\hbar_{\Gamma ZB}) - \\ &\quad 4(E-\hbar\omega_{ZB}-E_{\Gamma L})^{\frac{1}{2}}f(E)\Big\} \qquad (14)\end{aligned}$$

The occupation numbers f^X(and similarly for f^L) of the X valleys can be obtained by solving the rate equation:

$$\frac{df^X}{dt} = \left(\frac{\partial f^X}{\partial t}\right)_{X\leftrightarrow\Gamma} + \left(\frac{\partial f^X}{\partial t}\right)_{X\leftrightarrow L} + \left(\frac{\partial f^X}{\partial t}\right)_{\text{intravalley}} \qquad (15)$$

where $\left(\frac{\partial f^X}{\partial t}\right)_{X\leftrightarrow\Gamma}$ and $\left(\frac{\partial f^X}{\partial t}\right)_{X\leftrightarrow L}$ are respectively the rates due to intervalley scattering between the X valleys and the Γ valley and between the X valleys and the L valleys, and $\left(\frac{\partial f^X}{\partial t}\right)_{\text{intravalley}}$ is the rate due to

intra-X valley scattering via LO phonons. We have numerically solved the rate equations for f, f^X and f^L and found that the populations in the X and L valleys affect the nonequilibrium LO phonon population. The reason is that the population in these valleys will eventually return to the Γ valley, although the time it takes them to do so is of the order of the LO phonon lifetime so their contribution to the nonequilibrium LO phonon population is much reduced.

To summarize the most important effect of the higher X and L conduction minima is to syphon off electrons from the Γ valley at rates exceeding 10^{13} sec^{-1} and then return the electrons to the Γ valley at much slower rates ($\lesssim 10^{12} sec^{-1}$). The net effect on the optically excited LO phonon population is somewhat similar to that of broadening the excitation pulse but keeping the total energy constant. In Fig. 5 we show qualitatively the effect of including intervalley scattering in our parabolic bands model. The value of the intervalley deformation potentials used in this calculation are given in Table I.

D. Band Structure Effects

Finally we will consider the differences between the actual band structure of GaAs and the simple two parabolic band model and how these differences affect our results. These differences and their significance can be summarized as follows:

(1) Warping of the valence bands in GaAs cause a spread in the energy distribution of the photoexcited electrons.

(2) The nonparabolicity of the Γ_1 conduction band produces two effects. One effect is to increase the density of final states available in the LO

phonon scattering processes while the other is to change the photon energies for the onset of intervalley scatterings.

(3) It was pointed out by Rode[16] that the nonparabolicity of the Γ_1 conduction band results from the mixing of s-like Γ_1 wave functions with the p-like Γ_{15} wave functions via the $\bar{k}\cdot\bar{p}$ perturbation. It is therefore inconsistent to assume a nonparabolic conduction band with a s-like wave function. The admixture of p-like wave functions in the cnduction band changes the Fröhlich electron-LO phonon matrix element.

These band structure effects can all be adequately included in our calculation by using the Kane model[17] for the conduction and valence bands of GaAs. The exception is the prediction of the photon energy for the onset of the intervalley scattering processes. Since the Kane model is not accurate for large electron wave vectors where the intervalley scattering processes occur, we have to resort to a more complete band structure calculation to determine these onset energies. For this we have chosen the non-local empirical pseudopotential calculation of Chelikowsky and Cohen for GaAs.[11]

Within the Kane model the dispersion relationships for the heavy hole band and the conduction band can be written respectively as:

$$E_{hh}(K,\theta,\phi) = \{A - Bf(\theta,\phi)\}K^2 \tag{16}$$

and

$$E_c = \frac{\hbar^2K^2}{2m^*} - \frac{E_g}{2} + \sqrt{\left(\frac{E_g}{2}\right)^2 + \frac{\hbar^2K^2|P|^2}{m^*m_o}} \tag{17}$$

where

$$f(\theta,\phi) = [1 + \frac{C^2}{B^2}(\sin^2\theta\cos^2\theta + \sin^4\theta\cos^2\phi\sin^2\phi)]^{\frac{1}{2}} \tag{18}$$

A, B, and C are the valence band parameters introduced by Dresselhaus, Kip and Kittel[18], E_g is the energy gap, m^* is the electron effective mass

for small values of K, m_o is the free electron mass and $|P|^2$ is the matrix element of the electron momentum operator between the Γ_1 conduction band and the Γ_{15} valence band. The optically excited electron population f(K,t=0) due to transition from the heavy hole band to the conduction band is given by:

$$f(K,t=0) \propto \int \sin^2\theta d\theta d\phi \; |P(\theta,\phi)|^2 \rho_{hh}(K,\theta,\phi)\rho_c(K) \; \delta(E_g + E_{hh}(K,\theta,\phi) + E_c(K) - \hbar\omega_i) \tag{19}$$

where ρ_{hh} and ρ_c are respectively the density-of-states of the heavy-hole band and of the conduction band. Values of the band parameters in the Kane model can be found in Table I.

The non-parabolic conduction band as represented by Eq.(17) can be expressed alternately as

$$\frac{\hbar^2K^2}{2m^*} = \gamma(E_c) \simeq E_c + \alpha E_c^2 + \beta E_c^3 \tag{20}$$

where α and β can be shown to be approximately $0.577(eV)^{-1}$ and $0.047(eV)^{-2}$ respectively. The effect of this nonparabolicity on the intravalley scattering rate $\left(\frac{\partial f_K}{\partial t}\right)_{LO}$ and on the phonon generation rate $\left(\frac{\partial N_q}{\partial t}\right)_e$ are discussed in Appendix II. The results obtained are given by:

$$\left(\frac{\partial f(E)}{\partial t}\right)_{LO} = \frac{e\mathcal{E}_o}{\sqrt{2m^*\gamma(E)}} \left\{ \gamma'(E_+) \int_{\sqrt{\gamma(E_+)} - \sqrt{\gamma(E)}}^{\sqrt{\gamma(E_+)} + \sqrt{\gamma(E)}} [(N_q+1)f(E_+) - N_q f(E)] \frac{dq}{q} \right.$$

$$\left. + \gamma'(E_-) \int_{\sqrt{\gamma(E)} - \sqrt{\gamma(E_-)}}^{\sqrt{\gamma(E)} + \sqrt{\gamma(E_-)}} [N_q f(E_-) - (N_q+1)f(E)] \frac{dq}{q} \right\} \tag{21}$$

and $$\left(\frac{\partial N_{\bar{q}}}{\partial t}\right)_e = \frac{2em^*\mathcal{E}_o}{\hbar^3 q^3}\left\{(N_q+1)\int_{E_1(q)}^{\infty}\gamma'(E_-)\gamma'(E)f(E)dE - N_q\int_{E_2(q)}^{\infty}\gamma'(E_+)\gamma'(E)f(E)dE\right\} \tag{22}$$

where $\gamma' = \frac{d\gamma}{dE}$, $E_+ = E + \hbar\omega_{LO}$, $E_- = E - \hbar\omega_{LO}$ and $E_1(q)$ and $E_2(q)$ are defined in Appendix II. As pointed out by Conwell who obtained $\left(\frac{\partial f}{\partial t}\right)_{LO}$ in a different way the effect of band nonparabolicity on <u>inter</u>valley scattering is to change the density of states of the Γ valley. This only affects the calculation of $\left(\frac{\partial f}{\partial t}\right)_{X\leftrightarrow\Gamma}$ and $\left(\frac{\partial f}{\partial t}\right)_{L\leftrightarrow\Gamma}$. In both cases the only change needed is to replace the effective mass m* of the Γ_1 conduction band by $(m^*)^{3/2}\sqrt{\gamma(E)}\left(\frac{d\gamma}{dE}\right)$.

The effect of mixing between the Γ_1 conduction band and the Γ_{15} valence band wave functions on the Fröhlich matrix element $M_{\bar{K},\bar{K}'}$ can be taken care of simply by multiplying $M_{\bar{K},\bar{K}'}$ by an overlap integral $G(\bar{K},\bar{K}')$. It can be shown that $G(\bar{K},\bar{K}')$ can be expressed as:[16]

$$G(\bar{K},\bar{K}') = (a(\bar{K})a(\bar{K}') + c(\bar{K})c(\bar{K}')\cos\theta)^2 \tag{23}$$

where θ is the angle between $\bar{K}$ and $\bar{K}'$, a and c are two functions defined by the equations:

$$a^2(\bar{K}) = \frac{1}{2}\left(1 + \frac{(E_{g/2})}{\left[(E_{g/2})^2 + \frac{\hbar^2K^2|P|^2}{m_o^2}\right]^{1/2}}\right) \tag{24}$$

and $$a^2 + c^2 = 1 \tag{25}$$

By modifying $M_{\bar{K},\bar{K}'}$ in Eq.(3) and recalculating the integration over $\bar{q}$ we obtain in a strightforward manner (see Appendix III for details) the final

results:

$$\left(\frac{\partial f(E)}{\partial t}\right)_{LO} = \frac{e\mathcal{E}_o}{\sqrt{2m^*\gamma(E)}}\left\{\gamma'(E_+)f(E_+)\ln\left(\frac{\sqrt{\gamma(E_+)}+\sqrt{\gamma(E)}}{\sqrt{\gamma(E_+)}-\sqrt{\gamma(E)}}\right) \times\right.$$

$$\left(1-\frac{c(E)c(E_+)}{\ln\left(\frac{\sqrt{\gamma(E_+)}+\sqrt{\gamma(E)}}{\sqrt{\gamma(E_+)}-\sqrt{\gamma(E)}}\right)}\right) - \gamma'(E_-)f(E) \quad \times$$

$$\ln\left(\frac{\sqrt{\gamma(E)}+\sqrt{\gamma(E_-)}}{\sqrt{\gamma(E)}-\sqrt{\gamma(E_-)}}\right)\left(1-\frac{c(E)c(E_-)}{\ln\left(\frac{\sqrt{\gamma(E)}+\sqrt{\gamma(E_-)}}{\sqrt{\gamma(E)}-\sqrt{\gamma(E_-)}}\right)}\right) \quad (26)$$

$$\left(\frac{\partial N_q}{\partial t}\right)_c = \frac{2em^*\mathcal{E}_o}{\hbar^3 q^3}\int_{E_1(q)}^{\infty}\gamma'(E_-)\gamma'(E)f(E)dE -$$

$$\frac{e\mathcal{E}_o}{2\hbar q}\int_{E_1(q)}^{\infty}\frac{\gamma'(E_-)\gamma'(E)}{\gamma^{\frac{1}{2}}(E)\gamma^{\frac{1}{2}}(E_-)}c(E)c(E_-)f(E)dE \quad (27)$$

In Eq.(27) the second term is produced by admixture of the p-like wave functions. The net effect of this admixture is to <u>reduce</u> the number of LO phonon generated. But on the other hand, the nonparabolicity of the conduction band which also results from this admixture tend to <u>increase</u> the number of LO phonon generated so the two effects partially cancel. Also note the different q dependence in the two terms on the right hand side of Eq.(27). The first terms varies as q^{-3} while the second term due to the p-wave function admixture varies as q^{-1}. Therefore, the admixture term affects the large wave vector LO phonons more than the small q LO

phonons probed by Raman scattering. In Figure 5 we show the calculated LO phonon population N_{LO} after including all these band structure effects. The nonparabolicity of the conduction band produces two significant effects on N_{LO}. Firstly, it enhances N_{LO} for $\hbar\omega_i \geq 2.0$eV. Since we have normalized the two theoretical curves in Fig. 5 at $\hbar\omega_i = 2.0$eV this has produced a decrease in the value of N_{LO} in the region $\hbar\omega_i < 1.9$eV when nonparabolicity of the conduction band is included. Secondly, the nonparabolicity of the conduction band shifts the energy onset for Γ to X intervalley scattering from 2.08eV to ~ 2.11eV.

III. Experimental Setup and Results

The experimental setup we used to produce the picosecond, tunable laser pulses for exciting the nonequilibrium phonon in GaAs and to collect and analyze the Raman scattered light is shown in Fig. 6. An actively modelocked Ar ion laser (Spectra Physics Model 171) produces ~150 psec long pulses at ~82 MHz repetition rate and pumps synchronously a dye laser using either Rhodamine 6G or DCM as the lasing medium. The dye laser pulse lengths are monitored by an autocorrelator using a KDP crystal in a background free second harmonic generation arrangement.[19] Typically the autocorrelation traces indicate that the dye laser pulses are completely modelocked with full-width at half-maximum of ~4 psec. The output wavelength of the dye laser can be tuned continuously from ~720 nm to 575 nm by using the above two dyes.

The dye laser beam is passed through a pair of Brewster angle prisms to eliminate the dye fluorescence background before being focussed with an achromatic lens onto the GaAs sample cooled to ~10 K by He exchange gas

in a Janis optical dewar. The GaAs sample is a 4μ thick high purity epitaxial layer ($N_D - N_A \leq 10^{14} cm^{-3}$) grown on a semi-insulating subtrate obtained from Hewlett-Packard. The normal to the crystal surface is along the (100) direction. The incident laser is polarized along the (010) direction while the scattered radiation is polarized along the (001) direction. In this backscattering configuration the LO phonon is allowed by Raman selection rules while the TO phonon is not.[20] The scattered radiation is analyzed by a SPEX Model 1403 double monochromator and detected by a cooled RCA C31034 photomultiplier tube with standard photon counting electronics.

To determine the LO phonon population N_{LO} it is necessary to measure both the Stokes and anti-Stokes intensities. Since both the incident and scattered radiations are strongly absorbed by the sample, the Raman tensor $\tilde{R}_{xy}(\omega_i,\omega_s)$ can vary strongly with the incident and scattered photon frequencies (denoted by ω_i and ω_s respectively). As a result we can express the Stokes intensity $I_S(\omega_i,\omega_i-\omega_{LO})$ and anti-Stokes intensity $I_{AS}(\omega_i,\omega_i-\omega_{LO})$ as:

$$I_S(\omega_i,\omega_i-\omega_{LO}) \propto |\hat{e}_i \cdot \tilde{R}_{xy}(\omega_i,\omega_i-\omega_{LO}) \cdot \hat{e}_s|^2 \times [\alpha(\omega_i) + \alpha(\omega_i-\omega_{LO})]^{-1}(N_{LO} + 1) \tag{28}$$

and

$$I_{AS}(\omega_i,\omega_i+\omega_{LO}) \propto |\hat{e}_i \cdot \tilde{R}_{xy}(\omega_i,\omega_i+\omega_{LO}) \cdot \hat{e}_s|^2 N_{LO} \times [\alpha(\omega_i) + \alpha(\omega_i+\omega_{LO})]^{-1}. \tag{29}$$

In Eqs.(28) and (29) $\hat{e}_i$ and $\hat{e}_s$ are unit vectors along the polarizations of the incident and scattered radiations, $\alpha(\omega)$ is the absorption coefficient of GaAs at frequency ω. To correct for the dispersion in the Raman tensor we measured the Stokes intensity of the LO phonon using a low power cw dye

laser beam and we utilize the relationship:[21]

$$\tilde{R}_{xy}(\omega_i,\omega_i-\omega_{LO}) = \tilde{R}_{yx}(\omega_i-\omega_{LO},\omega_i) \tag{30}$$

which follows from time-reversal symmetry. This correction turned out to be relatively small (~5%) over the frequency range of our experiment. In addition to the dispersion of the Raman tensor the variation in the efficiency of the spectrometer and the photomultiplier $(Q(\omega))$ was also corrected for. This results in the final expression:

$$N_{LO}(\omega_i) = \left\{ \frac{Q(\omega_i+\omega_{LO})}{Q(\omega_i-\omega_{LO})} \left(\frac{\omega_i+\omega_{LO}}{\omega_i-\omega_{LO}}\right)^3 \left(\frac{\alpha(\omega_i)+\alpha(\omega_i-\omega_{LO})}{\alpha(\omega_i)+\alpha(\omega_i+\omega_{LO})}\right)\left(\frac{I_S}{I_{AS}}\right) \left|\frac{e_i \cdot \tilde{R}_{yx}(\omega_i+\omega_{LO},\omega_i) \cdot \hat{e}_s}{e_i \cdot \tilde{R}_{xy}(\omega_i,\omega_i-\omega_{LO}) \cdot \hat{e}_s}\right|^2 - 1 \right\}^{-1} \tag{31}$$

The resultant values of N_{LO} obtained in this way are displayed as closed circles in Figs. 3 and 5. The error bars around the experimental points mainly represent the uncertainties in the measurement of the Raman intensities and of the background due to dark counts and stray lights. The error bars are larger for $\hbar\omega_i < 1.95$eV because the dye laser output is more noisy when the dye DCM is used.

From Fig. 5 it is clear that the measured population of the LO phonon in GaAs is many order of magnitudes larger than that of the thermal equilibrium value of $\sim 10^{-18}$ at a lattice temperature of 10 K. To make sure that this high phonon population is not produced by local heating of the sample due to the focussed laser beam, we performed the following tests. First we measured the time integrated luminescence spectrum of the sample under the same conditions as the Raman measurements. This is shown in Fig. 7. The width of this spectrum indicated that the sample temperature was $\lesssim$ 15 K in good agreement with the reading of the diode thermometer on

the sample block. The peak poisiton of the LO phonon was determined to be 298±2 cm^{-1} and from the known temperature dependence of the LO phonon Raman peak[22] we estimated the sample temperature to be <50 K. In the third test the modelocker on the Ar^+ laser was turned off and a cw dye laser beam with the same average power as the modelocked beam was used to measure the Raman spectra. In this case no anti-Stokes signal was observable. This suggested that the LO phonon were not generated by sample heating since the heating would depend only on the average power of the laser beam. On the otherhand if the phonons were generated by optical pumping then the phonon generation rate when the laser was cw would be reduced from the rate when the laser was modelocked by a factor given by the ratio of the pulse length (~4 psec) to the pulse separation (~12 nsec). Since this ratios is $<10^{-3}$ we do not expect to observe any anti-Stokes signal when the laser is cw. As a final test we repeated the optical pumping experiment on a GaAs sample oriented with its surface normal to the (110) direction. For this orientation the TO phonon was allowed by Raman selection rule.[20] Under identical laser conditions where a strong anti-Stokes LO phonon was observed (see Fig. 8(a) and (b)) we found no significant anti-Stokes intensities for the TO phonon (see Fig. 8(c) and (d)). This is consistent with the fact that there is negligible sample heating by the modelocked dye laser and that the TO phonons in GaAs do not couple to the electrons as strongly as the LO phonons.

IV. Comparison Between Theory and Experiment

In the theoretical claculations presented in Section II we have assumed that the incident radiation is a delta function both in photon

energy and time. Since the dye laser spectral width is only ~1 cm^{-1} this assumption of the incident radiation being a delta function in energy is justifiable. This is, however, not true for the assumption involving time since the dye laser pulses are ~4 psec wide. Because of the finite pulse width the scattered intensities I_S and I_{AS} are not necessarily proportionally to $N_{LO}+1$ and N_{LO} where N_{LO} is the LO phonon population calculated by assuming a delta function excitation pulse. Instead we have to calculate the phonon population N^*_{LO} for the laser profile $I_i(t)$. Because the generation time of the LO phonons by the cascade processes is only ~0.1 psec the time dependence of the LO phonon population is determined by the laser pulse via:

$$N^*_{LO}(t) = \int_{-\infty}^{\infty} N_{LO}(t-\tau) I_i(\tau) d\tau \tag{32}$$

Since Raman scattering is an instantaneous process the measured Stokes Raman intensity results from the convolution of N^*_{LO} and I_i:

$$I_S \propto \int_{-\infty}^{\infty} N^*_{LO}(t) I_i(t) dt \tag{33}$$

Thus the net effect of a broader laser pulse is to reduce I_S by a constant factor provided the laser profile is unchanged as the dye laser frequency is varied. For a Gaussian pulse of full-width at half-maximum of 4 psec this factor turns out to be ~0.4. Since the injected carrier densities have uncertainties of similar orders of magnitude, we have normalized the theoretical and measured values of N_{LO} at $\hbar\omega_i$ ~ 2.0eV by adjusting the density of injected carriers.

Figure 5 shows a comparison between the experimental results (solid circles) and the theoretical results based on two parabolic band models. In one case the phonon wave vector probed by Raman scattering is assumed

to be constant and equal to $7.0\times10^5 cm^{-1}$ while in the other case it is assumed to be determined by the incident photon wavevectors. The carrier density assumed in the two cases are respectively $3.4\times10^{15} cm^{-3}$ and $4.8 \times 10^{15} cm^{-3}$. It is clear that the experimental values of N_{LO} show a saturation as $\hbar\omega_i$ becomes larger than 1.95eV which is not reproduced by the constant q model. Although the varying q model reproduces this saturation, it also deviates from the experimental result in two respects. First, the slope of the increase in N_{LO} with $\hbar\omega_i$ between 1.75 and 1.9eV is different between theory and experiment. Second, the theoretical curve does not show the sudden drop in the value of N_{LO} at ~2.1eV.

Since this drop in N_{LO} at ~2.1eV is due to the presence of higher conduction band minima near the X points of the Brillouin zone, the parabolic band model is augmented by assuming that there are now higher energy minima at the L points and X points with respective energies $E_{\Gamma L}$ and $E_{\Gamma X}$ above the Γ minimum. The values of $E_{\Gamma L}$, $E_{\Gamma X}$ and the intervalley deformation potentials $D_{\Gamma X}$, $D_{\Gamma L}$ and D_{LX} given in Table I are used in the calculation. The resultant curve is compared with the experimental results in Fig. 5. We note that the Γ to L scattering only slightly decreases the value of N_{LO} above 1.95eV. On the other hand, the Γ to X intervalley scattering produces a drop in N_{LO} comparable to the experimental result although at the wrong photon energy.

To account for the stronger increase in N_{LO} with $\hbar\omega_i$ than predicted by the parabolic band models we consider a nonparabolic band model in which the band parameters are obtained from a realistic band structure calculation. The resultant curve is compared with the experimental results in Fig. 6. The nonparabolicity of the conduction band has several

significant effects. At $\hbar\omega_i < 1.9$eV the theoretical curve based on nonparabolic band is much steeper than the curve based on parabolic bands. This is understandable since for $\hbar\omega_i \leq 1.9$eV the conduction band wave vectors involved are already large enough for nonparabolic effects to be important. Also the nonparabolicity shifts the onset in the decrease in N_{LO} due to Γ-X scattering up to $\hbar\omega_i = 2.105$eV in excellent with the experimental result. Since the nonparabolicity also causes the generation rate of LO phonons to increase, it is necessary to adjust the value of $D_{\Gamma X}$ upwards to fit the decrease in N_{LO} observed experimentally. The solid theoretical curve in Fig. 6 was obtained with the following values for the intervalley deformation potentials:

$$D_{\Gamma X} = (11 \pm 1) \times 10^8 \text{eV/cm}$$

$$D_{\Gamma L} \leq 1.5 \times 10^8 \text{eV/cm}$$

$$D_{XL} = (2.75 \pm 0.2) \times 10^8 \text{eV/cm}.$$

The value of $D_{\Gamma X}$ we determined is in excellent agreement with the value deduced from Gunn effect measurements.[23] Our value of $D_{\Gamma L}$ is smaller than the Gunn effect value, although our value is consistent with the value of $D_{\Gamma L} \simeq 1.5\times10^8$eV/cm determined by Koch et al.[24] from optically pumped laser action in highly excited GaAs. Also our values of the deformation potentials are all in good agreement with the values deduced by Pozela and Reklaitis[25] from analyzing the high field drift velocity and longitudinal diffusion coefficients of GaAs by Monte Carlo calculation. This is not surprising since our technique is much more sensitive to the Γ→L scattering than Gunn effect. The reason is because by choosing our photon energy appropriately (i.e., $1.9\text{eV} \leq \hbar\omega_i \leq 2.1\text{eV}$) we can inject electrons with sufficient energy to scatter only into the L minima but not into the X minima.

Finally, it is interesting to note that the width of the decrease in N_{LO} at $\hbar\omega_i$ = 2.105eV reflects mainly the finite width of the electron energy distribution which results from the warping of the heavy hole band. If the electron distribution has been assumed to be a delta function then the drop in N_{LO} will occur with a width of about 0.01eV. Including the warping of the valence band increased this width to more than 0.03eV in very good agreement with experiment.

V. Discussions and Conclusions

We have demonstrated that nonequilibrium LO phonons produced by the relaxation of hot electrons excited by above band gap radiation can be utilized to study band structures of semiconductors. Since this technique is a form of spectroscopy similar to photoacoustic spectroscopy, we have labelled this technique nonequilibrium phonon spectroscopy in an earlier publication.[10]

It is worth while to compare the two techniques to determine their similarities and differences. In both techniques radiation incident on a sample is absorbed by electrons which then transfer the energy to phonons so both techniques can be utliized to measure absorption coefficients. In photoacoustic spectroscopies the energy imparted to the phonons by the electrons is detected in the form of a strain wave or heat or any other heat produced effects in the sample. The advantage of these detection schemes is their high sensitivity and as a result photoacoustic spectroscopies have been utilized to measure very small absorption coefficients. However, the process of converting energy into acoustic phonons and heat requires microseconds or longer so photoacoustic spectroscopies are not

suited to study fast processes. In the present technique we do not have to wait for the electron energy to be transfered to acoustic phonons; instead we monitor the LO phonon population produced by the relaxing electrons. Since the LO phonon emission processes occur in ~0.1 psec our technique has very fast response time. However, the Raman scattering technique we rely on to measure the LO phonon population has very low sensitivity and requires keeping the sample at low temperature to minimize the amount of thermally excited optical phonons. Part of the poor sensitivity of Raman scattering results from the fact that only phonons satisfying momentum conservation are detected. So far in interpreting photoacoustic spectra it has generally been assumed that the efficiency with which energy absorbed by electrons are converted into acoustic phonons is independent of the photon energy. We have shown that this is far from being the case for the LO phonons. If the efficiency in the creation of LO phonons by energetic electrons were indeed independent of the photon energy, the experimental nonequilibrium LO phonon population will follow the absorption curve. The fact that the experimental results in Fig. 5 show strong structures due to intervalley scattering indicates that nonequilibrium phonon spectroscopy can be exploited to study indirect energy gaps and intervalley electron-phonon interactions. Other possible applications of this technique include the study of non-radiative recombination of photoexcited carriers at deep centers via multi-phonon emission.[26]

In summary we have excited a nonequilibrium longitudinal phonon population in GaAs by means of above band-gap picosecond dye laser pulses. Using Raman scattering to monitor the LO phonon population as a function of the incident photon energy we demonstrated that this is a new

spectroscopic technique which can be applied to study indirect energy gaps above the fundamental gap and also ultrafast intervalley electron-phonon scatterings occurring in times less than 10^{-13}sec.

Acknowledgements

We are grateful to S.G. Louie and M. Hybertson for providing us with band parameters of GaAs which they obtained from pseudopotential calculations. GaAs samples from Hewlett-Packard of Palo Alto and technical assistance from F. Askary are also gratefully acknowledged. This work is supported by the Director, Office of Energy Reserach, Office of Basic Energy Sciences, Materials Sciences Divison of the U.S. Department of Energy under Contract Number DE-AC03-76SF00098.

References

1. See for example E.M. Conwell, in High Field Transport in Semiconductors, Solid State Physics: Advances in Research and Applications, edited by F. Seitz (Academic Press, New York, 1967) Suppl. 9.
2. E.M. Conwell and M.O. Vassel, IEEE-Trans. on Elect. Devices ED-13, 22 (1966).
3. R.J. Nicholas, A.C. Carter, S. Fung, R.A. Stradling, J.C. Portal and C. Houlbert, J. Phys. C 13, 5215 (1980).
4. R. Ulbrich, Phys. Rev. Letters 27, 1512 (1971).
5. J. Shah, R.C.C. Leite and J.F. Scott, Solid State Commun. 8, 1089 (1970).
6. J.C.V. Mattos and R.C.C. Leite, Solid State Commun. 12, 465 (1973).
7. D. von der Linde, J. Kuhl and H. Klingenburg, Phys. Rev. Lett. 44, 1505 (1980).
8. K.T. Tsen, D.A. Abramsohn and R. Bray, Phys. Rev. B26, 4770 (1982).
9. Y.B. Levinson and B.N. Levinsky, Solid State Commun. 16, 713 (1975).
10. Summaries of our results have been reported in C.L. Collins and P.Y.Yu, Phys. Rev. B 27, 2602 (1983), and Physica 117B & 118B, 286 (1983).
11. For a description of the band structure of GaAs see J.R. Chelikowsky and M.L. Cohen, Phys. Rev. Letters 32, 674 (1974) and J.R. Chelikowsky, Ph.D. Thesis (University of California, Berkeley, 1975, unpublished).
12. See for example review article by I.B. Levinson, Soviet Phy. Semiconductor 7, 1121 (1974) [Fiz. Tekh. Poluprov., 7, 1673 (1973)].
13. Although the conduction band minima along the [100] directions in GaAs occur slightly away from the X points of the Brillouin zone, we

will neglect this minor complication and refer to these minima as the X point valleys. See for example A. Pinczuk, S.G. Louis, B. Welber, J.C. Tsang and J.A. Bradley in Physics of Semiconductors, 1978, ed. by B.L.H. Wilson (Institute of Physics, Bristol and London, 1978) p. 1191.

14. R. Ulbrich, Phys. Rev. B8, 5719 (1973). It was shown that about 70% of the excess energy goes to the electrons.

15. J.L. Birman, M. Lax and R. Loudon, Phys. Rev. 145, 620 (1966).

16. D.L. Rode in Semiconductors and Semimetals, Vol. 10, ed. by R.K. Willardson and A.C. Beer (Academic Press, New York, 1975) Chapter 1.

17. E.O. Kane, in Semiconductors and Semimetals, Vol. 1, ed. by R.K. Willardson and A.C. Beer (Academic Press, New York, 1966).

18. See for example C. Kittel, Quantum Theory of Solids, (J. Wiley & Sons, Inc., New York, 1963) p. 273.

19. See article by E.P. Ippen and C.V. Shank in Ultrashort Light Pulses, Topics in Applied Physics, Vol. 18, ed. by S.L. Shapiro (Springer-Verlag, Berlin, 1977).

20. R. Loudon, Adv. in Phys. 13, 423 (1964).

21. W. Hayes and R. Loudon, Scattering of Light by Crystals (Wiley Interscience, New York, 1978) p. 25.

22. J.M. Ralston, D.E. Keating and R.K. Chang, Light Scattering Spectra of Solids, ed. by G. B. Wright (Plenum, New York, 1968) p. 369.

23. P.J. Vinson, C. Pickering, R.A. Adams, W. Fawcett and G.D. Pitt, Proc. of the 13th International Conf. on the Physics of Semiconductors, ed. by F.G. Fumi (Tipogravia, Rome, 1976) p. 1243.

24. T.L. Koch, L.C. Chin, Ch. Harden and A. Yariv, App. Phys. Lett. 41, 6 (1982).

25. J. Pozela and A. Reklaitis, Solid State Electronics 23, 927 (1980).

26. See for example C.H. Henry and D.V. Lang, Proc. of the Twelth Int. Conf. on the Physics of Semiconductors, ed. by M.H. Pilkuhn (B.G. Teubner, Stuttgart, 1974) p. 411.

TABLE I

Relevant Material Parameters of GaAs

1. Phonon Energies[a]

Symmetry	Phonon Energy (meV)
TO(Γ), LO(Γ)	33.8, 37
TO(L), LO(L)	34.4, 31.1
TA(L), LA(L)	8.1, 27
LO(X)	31.1

2. Band Parameters

Band gap $E_g = 1.519$ eV[b]

spin-orbit splitting $\Delta_o = 0.341$ eV[b]

$E_{\Gamma X} = 0.46$ eV[c]

$E_{\Gamma L} = 0.29$ eV[c]

Γ_1 conduction band effective mass $= 0.067\ m_o$[b]

Density-of-states mass for one X valley $= [m_x^X m_y^X m_z^X]^{1/3} = 0.407m$[d]

Density-of-states mass for one L valley $= [m_x^L m_y^L m_z^L]^{1/3} = 0.22m_o$[d]

Γ_{15} Valley Band Parameters[e]: $-A = 7.63$ (in units of $\hbar^2/2m_o$)

$-B = 4.86$ (in units of $\hbar^2/2m_o$)

$C^2 = 56.7$ (in units of $(\hbar^2/2m_o)^2$)

Electron Momentum Matrix Element, $\frac{|P|^2}{2m_o}$, between Γ_1 conduction band and Γ_{15} valence band = 25.7 eV[f]

3. Deformation Potentials for Intervalley Electron-Phonon Scattering

$D_{\Gamma X} = 10\times10^8$ eV/cm

$D_{\Gamma L} = 1.5\times10^8$ eV/cm

$D_{\Gamma X} = 2.75\times10^8$ eV/cm

Table I (cont'd)

4. Other Parameters[b]

$\varepsilon_\infty = 10.9$

$\varepsilon_o = 12.8$

Density = 5.3 gm/cm^3

- - - - - - - - - - - -

(a) G. Dolling and J.L.T. Waugh, Lattice Dynamics (Pergamon Press, Oxford, 1967) p. 19.

(b) M. Neuberger, III-V Semiconducting Compounds (IFI/Plenum, New York, 1971).

(c) D.E. Aspnes, C.G. Olsen, D.W. Lynch, Phys. Rev. Lett. 37, 766 (1976).

(d) Ref. 11.

(e) J.D. Wiley in Semiconductors and Semimetals Vol. 10, ed. by R.K. Willardson and A.C. Beer (Academic Press, New York, 1975) Chapter 2.

(f) P. Lawaetz, Phys. Rev. B4, 3460 (1971).

Figure Captions

Fig. 1 Schematic two parabolic bands model of GaAs showing the relaxation of photoexcited electrons via a cascade of emission of LO phonons.

Fig. 2 A plot of the LO phonon population versus phonon wave number about 3 psec after the sample has been excited by a 6 psec long dye laser pulse with photon energy $\hbar\omega = 1.77$eV.

Fig. 3 Nonequilibrium phonon occupation number observed by Raman scattering versus incident photon energy as calculated with a two parabolic bands model under two different assumptions. In one case the phonon wave vector Q is assumed to be constant while the photoexcited carrier density is assumed to be $3.4\times10^{15}\text{cm}^{-3}$. In the second case the phonon wave vector is determined by the incident photon and the excited carrier density is increased to $4.8\times10^{15}\text{cm}^{-3}$. The solid circles are experimental results.

Fig. 4 Schematic parabolic conduction bands model of GaAs which includes intervalley scattering.

Fig. 5 Comparison between experimental nonequilibrium phonon occupation number (solid circles) and theoretical results based on either a parabolic band model (broken curves) or a nonparabolic band model. Note how the nonparabolicity of the conduction band affects the onset of the Γ-X intervalley scattering.

Fig. 6 Experimental setup for the generation and detection of nonequilibrium phonons in GaAs.

Fig. 7 Typical time integrated luminescence spectrum of an GaAs sample under picosecond pulse excitations. An analysis of this spectra suggested that the sample temperature is < 15 K.

Fig. 8 (a) and (b) show the Stokes and anti-Stokes LO phonon Raman spectra of GaAs we obtained with picosecond laser pulses. (c) and (d) show the Stokes and anti-Stokes TO phonon Raman spectra of GaAs obtained under similar conditions. The strong presence of the LO phonon in the anti-Stokes spectrum and the absence of the TO phonon in the anti-Stokes spectrum indicated that the LO phonons are not thermally excited.

Appendix I

In this appendix we will obtain exact solutions to Eqs. (10) and (11) subject to the initial condition that the electron generating function is given by:

$$G(E,t) = N_T \delta(E-E_n)\delta(t) \tag{A.1}$$

where N_T is the total number of electrons excited by the laser pulse. Because of energy conservation the electrons can be scattered into a set of discrete energy levels only. As a result we obtain

$$f(E,t) = \sum_{m=0}^{n} N_m(t)\delta(E - m\hbar\omega_{LO}-\Delta) \tag{A.2}$$

and

$$\frac{df(E,t)}{dt} = \sum_{m=0}^{n} \frac{dN_m(t)}{dt} \delta(E - m\hbar\omega_{LO}-\Delta) \tag{A.3}$$

where the integer n is determined by the condition that $0 \leq (E_{n-n}\hbar\omega_{LO}) < \hbar\omega_{LO}$. Substituting these expressions into Eq. (10) and assuming $(E) = \infty$ we can rewrite Eq. (10) as:

$$\begin{aligned}\sum_{m=0}^{n-1} \frac{dN_m}{dt} \delta(E-m\hbar\omega_{LO}-\Delta) &= \sum_{m=0}^{n-1} g_1(E)N_{m+1}\delta(E-m\hbar\omega_{LO}-\Delta) \\ &- \sum_{m=0}^{n} g_2(E)N_m\delta(E-m\hbar\omega_{LO}-\Delta) \\ &+ N_T\delta(E-E_n)\delta(t)\end{aligned} \tag{A.4}$$

where we have defined

$$g_1(E) = \frac{e\mathcal{E}_o}{2m^*E}\,\ell n\left(\frac{\sqrt{E_+}+\sqrt{E}}{\sqrt{E_+}-\sqrt{E}}\right)$$

$$g_2(E) = \frac{E_-}{E}\,g_1(E_-),$$

$E_+ = E+\hbar\omega_{LO}$ and $E_- = E - \hbar\omega_{LO}$.

By integrating (A.4) over E around $m\hbar\omega_{LO}+\Delta$ (for $1<m<n-1$) we obtain

$$\frac{dN_m(t)}{dt} = g_1(E_m)N_{m+1}(t) - g_2(E_m)N_m(t) \tag{A.5}$$

where $E_m = E_n - (n-m)\hbar\omega_{LO} = m\hbar\omega_{LO} + \Delta.$

Eq. (A.5) can be solved by assuming solutions of the form:

$$N_m(t) = \sum_{\ell=0}^{n-m} A_\ell^{n-m}\, e^{-g_2(E_{n-\ell})t} \qquad (0<m<n) \tag{A.6}$$

Substituting the expression (A.6) into Eq. (A.5) we obtain this recursion relation for the coefficients A_ℓ^{n-m} :

$$A_\ell^{n-m} = \frac{g_1(E_m)A_\ell^{n-m-1}}{g_2(E_m)-g_2(E_{n-\ell})}\,, \qquad 0 \leqslant \ell \leqslant n-m \tag{A.7}$$

The initial condition $N_m(0) = N_T\delta_{nm}$ translates into: $A_o^o = N_T$ and $\sum_{\ell=0}^{n-m} A_\ell^{n-m} = 0$. These two equations combined with (A.7) enables all the coefficients A_ℓ^{n-m} to be calculated and hence f(E,t) and N_q.

Appendix II

In this appendix we will examine the effect of the nonparabolicity of the conduction band on the electron-LO phonon scattering rates. We will first consider $\left(\frac{\partial N_{\bar{q}}}{\partial t}\right)_e$ by rewriting Eq. (4) as

$$\left(\frac{\partial N_q}{\partial t}\right)_e = \frac{V}{(2\pi)^2\hbar} \int_0^\infty f_K \, M_q K^2 dK \int_0^{2\pi} d\phi \int_0^\pi \sin\theta d\theta \times$$

$$[(N_{\bar{q}}+1)\,\delta\,(E_{\bar{K}} - E_{\bar{K}-\bar{q}} - \hbar\omega_{LO}) - N_q \delta(E_{\bar{K}} - E_{\bar{K}+\bar{q}} + \hbar\omega_{LO})] \qquad (A.8)$$

where the matrix element $M_q = \frac{2\pi\hbar^2 e\mathcal{E}_o}{Vm^* q^2}$ is assumed to be given by the same expression as Eq.(6) for a s-like conduction band. We first perform the integration over θ by noting that without loss of generality we can assume the z-axis to be parallel to $\bar{q}$ and θ is the angle between $\bar{q}$ and $\bar{K}$.

Let us first express the nonparabolic conduction band as:

$$\frac{\hbar^2 K^2}{2m^*} = \gamma(E) \qquad (A.9)$$

where $\gamma(E)$ can be approximated by

$$\gamma(E) = E + 0.577\ E^2 + 0.047\ E^3 \qquad (A.10)$$

and E is in units of eV. As $E_{\bar{K}\pm\bar{q}}$ is the only term in the delta functions in (A.10) which depends on $\cos\theta$ it can be shown easily that

$$\int_0^\pi \sin\theta\,\delta(E_{\bar{K}} - E_{\bar{K}\pm\bar{q}} \pm \hbar\omega_{LO})d\theta = \sum_i \frac{1}{\left|\left(\frac{dE_{\bar{K}\pm\bar{q}}}{d\cos\theta}\right)_{\theta_i}\right|} \qquad (A.11)$$

where θ_i are the poles of $E_{\bar{K}} - E_{\bar{K}\pm\bar{q}} \pm \hbar\omega_{LO}$ respectively.

Using (A.9) we can write

$$\frac{dE_{\bar{K}\pm\bar{q}}}{d\cos\theta} = \frac{\hbar^2 Kq}{m^*} \frac{1}{\left(\frac{d\gamma}{dE}\right)_{E_{\bar{K}\pm\bar{q}}}} \tag{A.12}$$

Next we have to calculate the poles of $E_{\bar{K}} - E_{\bar{K}\pm\bar{q}} \pm \hbar\omega_{LO}$. To do this we will use the fact that the wave vector q we can observe in Raman scattering is typically small compared to $\bar{K}$ so we can approximate

$$E_{\bar{K}\pm\bar{q}} \simeq E_{\bar{K}} + \frac{dE_{\bar{K}}}{dK^2}(q^2 \pm 2Kq\cos\theta) \tag{A.13}$$

and obtain the poles $\theta_\pm$:

$$\cos\theta_\pm \cong \frac{1}{2Kq}\left[\frac{2m^*\omega_{LO}}{\hbar}\left(\frac{d\gamma}{dE}\right) \mp q^2\right] \tag{A.14}$$

Using these results the integration over θ in (A.18) can be carried out. The final expression for $\left(\frac{\partial N_q}{\partial t}\right)_e$ we obtain is:

$$\left(\frac{\partial N_q}{\partial t}\right)_e = \frac{2em^*\mathcal{E}_o}{\hbar^3 q^3}\left\{(N_q+1)\int_{E_1(q)}^{\infty}\gamma'(E_-)\gamma'(E)f(E,t)dE - N_q\int_{E_2(q)}^{\infty}\gamma'(E_+)\gamma'(E)f(E,t)dE\right\} \tag{A.15}$$

where $E_1(q)$ and $E_2(a)$ are defined by the differential equations:

$$\gamma(E_1) = \frac{1}{4E_q}[\gamma'(E_1)\hbar\omega_{LO}+E_q]^2 \tag{A.16}$$

$$\gamma(E_2) = \frac{1}{4E_q}[\gamma'(E_2)\hbar\omega_{LO} - E_q]^2 \tag{A.17}$$

and $\gamma' = \frac{d\gamma}{dE}$. $\left(\frac{\partial f}{\partial f}\right)_{LO}$ can be obtained in a similar manner.

Appendix III

In this appendix we will calculate $\left(\frac{\partial N_{\bar{q}}}{\partial t}\right)_e$ again but now assuming that the Fröhlich matrix element M_q is modified by the admixture of p-like wave functions in the conduction band. As pointed out in Section II.D this is accomplished simply by multiplying M_q by an overlap integral

$$G(\bar{K},\bar{K}') = \left(a(K)a(K') + c(K)c(K')\cos\phi\right)^2$$

By assuming that stimulated emission of phonons is negligible we can express $\left(\frac{\partial f_K}{\partial t}\right)_{LO}$ as:

$$\left(\frac{\partial f_K}{\partial t}\right)_{LO} = \frac{VM_q}{2\pi\hbar}\left\{\int_0^\infty dq \int_0^\pi f(K_+)\left[a(K_+)a(K) + \frac{c(K)c(K_+)(K+q\cos\theta)}{K_+}\right]\delta(E_{K_+} - E_K - \hbar\omega_{LO})\sin\theta d\theta\right.$$

$$\left. - \int_0^\infty f(K)dq \int_0^\pi\left[a(K_-)a(K) + \frac{c(K)c(K_-)(K-q\cos\theta)}{K_-}\right]\delta(E_{K_-} - E_K + \hbar\omega_{LO})\sin\theta d\theta\right\} \tag{A.18}$$

where $K_\pm = |K\pm q| = [K^2 + q^2 \pm 2Kq\cos\theta]^{\frac{1}{2}}$.

The integral over θ can be essentially evaluated in the same way as in Appendix II. It is convenient to define a wave vector Q as:

$$Q^2 = \frac{2m^*\omega_{LO}}{\hbar} \frac{d\gamma}{dE} \tag{A.19}$$

so that the poles $\theta_\pm$ can be expressed as:

$$2Kq\cos\theta_\pm \simeq Q^2 \mp q^2 \tag{A.20}$$

At these poles $K_\pm$ can be written as

$$K_\pm\Big|_{\theta_\pm} = \sqrt{K^2 \pm Q^2} \tag{A.21}$$

Note that $K_\pm\Big|_{\theta_\pm}$ no longer depends on q and $\frac{\hbar^2}{2m^*}\left(K_\pm\Big|_{\theta_\pm}\right)^2 = \gamma(E_\pm) = \gamma(E_K \pm \hbar\omega_{LO})$. As a result we will denote $f(K_+\Big|_{\theta_+})$ by $f(E_+)$, $a(K_\pm\Big|_{\theta_\pm})$ and $c(K_\pm\Big|_{\theta_\pm})$ by $a(E_\pm)$ and $c(E_\pm)$. With these notations Eq.(A.18) after integration over θ can be written as

$$\left(\frac{\partial f_K}{\partial t}\right)_{LO} = \frac{VM_q}{2\pi\hbar}\left\{\int_{-K+\sqrt{K^2+Q^2}}^{K+\sqrt{K^2+Q^2}} f(E_+)\left[a(E_+)a(E)+c(E)c(E_+)\sqrt{\frac{\gamma(E)}{\gamma(E_+)}}\right] \times \right.$$

$$\frac{m^*\gamma'(E_+)}{\hbar^2 Kq}\,dq - \int_{K-\sqrt{K^2-Q^2}}^{K+\sqrt{K^2-Q^2}} f(E)\left[a(E_-)a(E)+c(E_-)c(E) \times\right.$$

$$\left.\sqrt{\frac{\gamma(E)}{\gamma(E_-)}}\right]\frac{m^*\gamma'(E_-)}{\hbar^2 Kq}\,dq \;+$$

$$\int_{-K+\sqrt{K^2+Q^2}}^{K+\sqrt{K^2+Q^2}} f(E_+)c(E)c(E_+)\left[\frac{\hbar^2(Q^2-q^2)}{4m^*\gamma^{\frac{1}{2}}(E)\gamma^{\frac{1}{2}}(E_+)}\right]\left[\frac{m^*\gamma'(E_+)}{\hbar^2 Kq}\right]dq \;-$$

$$\left.\int_{K-\sqrt{K^2-Q^2}}^{K+\sqrt{K^2-Q^2}} f(E)c(E)c(E_-)\left[\frac{\hbar^2(Q^2+q^2)}{4m^*\gamma^{\frac{1}{2}}(E)\gamma^{\frac{1}{2}}(E_-)}\right]\left[\frac{m^*\gamma'(E_-)}{\hbar^2 Kq}\right]dq\right\} \tag{A.22}$$

After integration over q and using the approximation $a(E)a(E_+)+c(E)c(E_+) \approx a(E)a(E_-)+c(E)c(E_-) \approx 1$ we obtain Eq. (26).

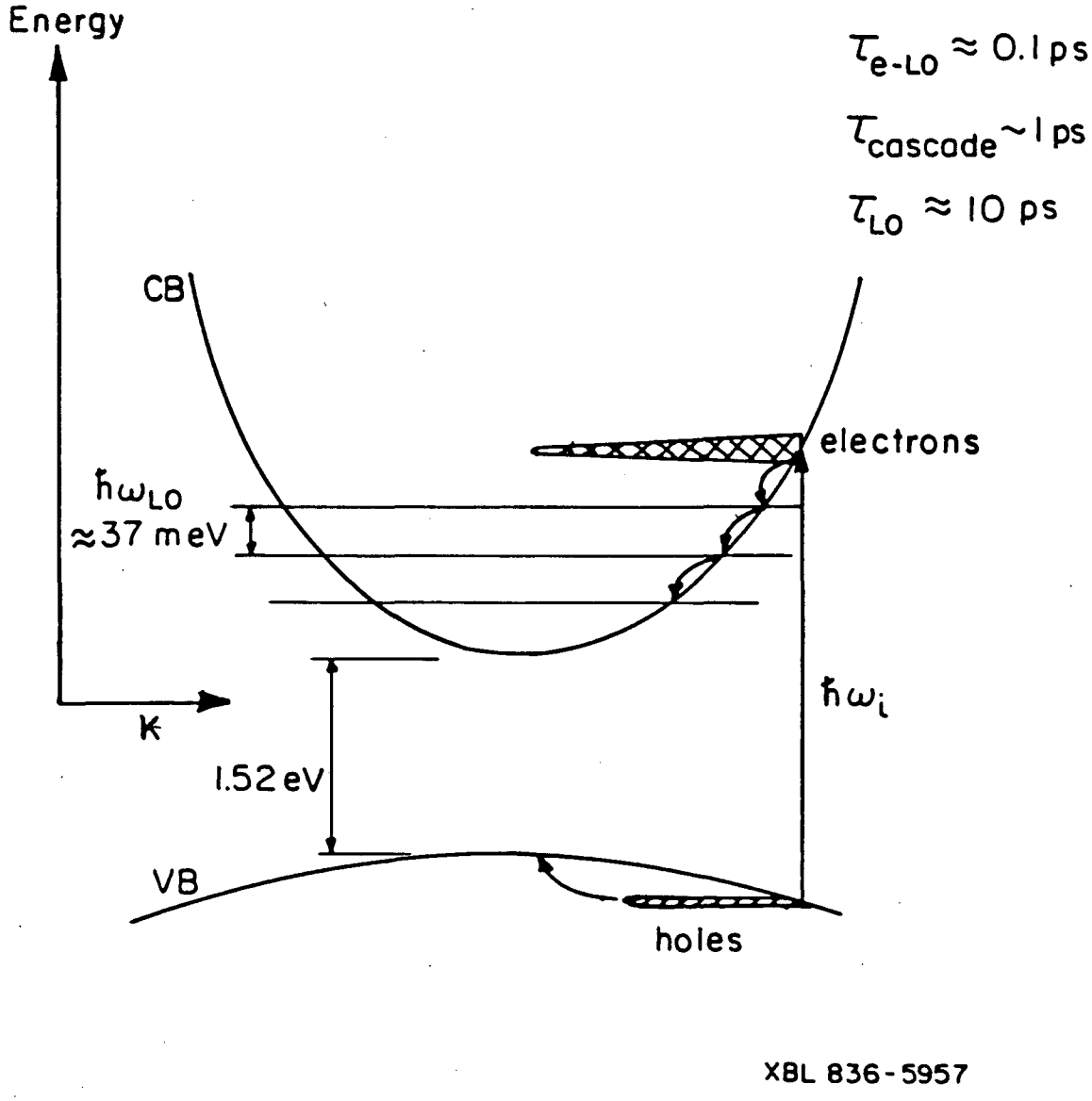
Energy
$\tau_{e\text{-}LO} \approx 0.1$ ps
$\tau_{cascade} \sim 1$ ps
$\tau_{LO} \approx 10$ ps
CB
electrons
$\hbar\omega_{LO}$
≈ 37 meV
$\hbar\omega_i$
K
1.52 eV
VB
holes
XBL 836-5957

Figure 1

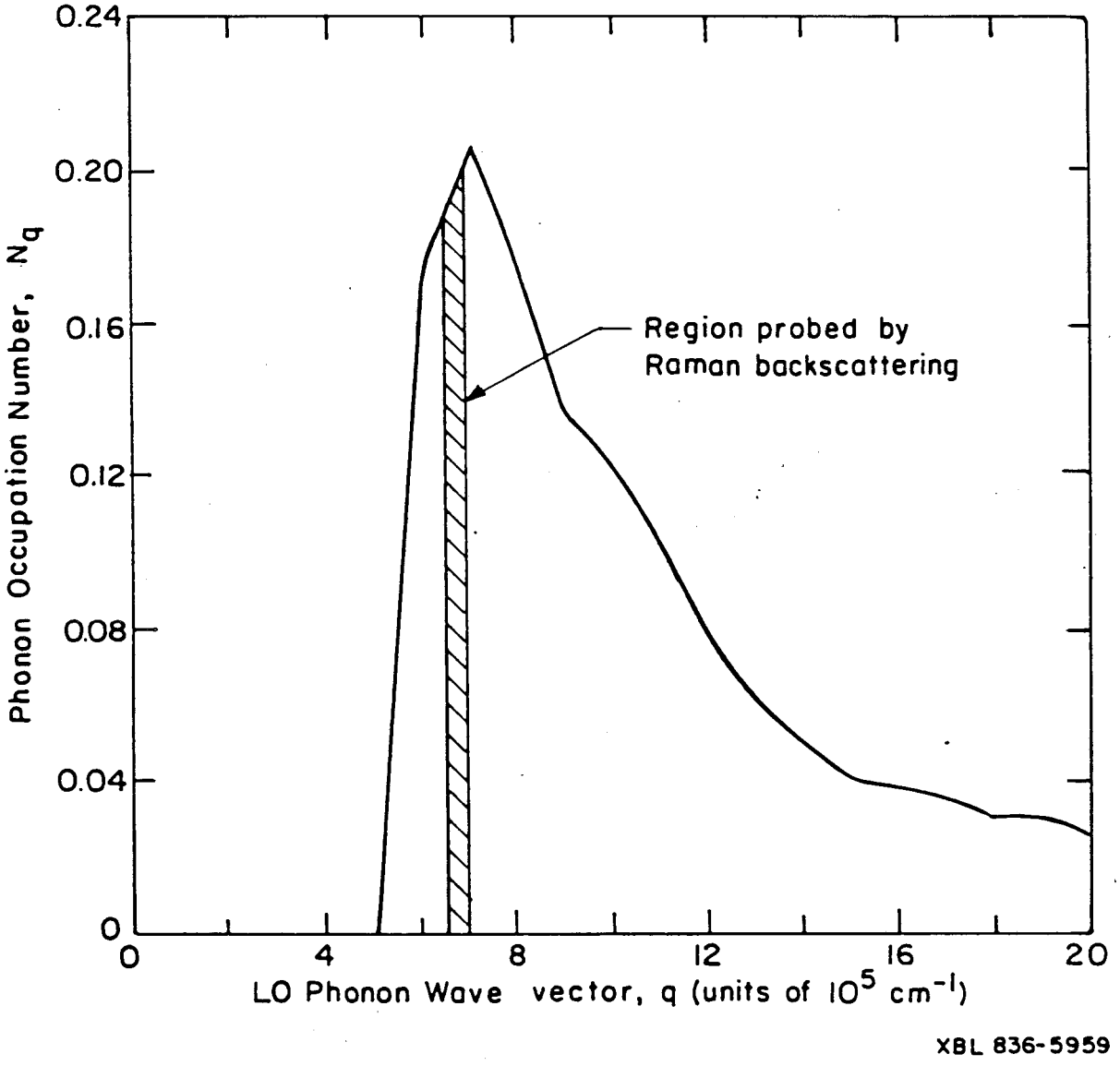
0.24
0.20
0.16
0.12
0.08
0.04
0
Phonon Occupation Number, N_q
Region probed by
Raman backscattering
0
4
8
12
16
20
LO Phonon Wave vector, q (units of 10^5 cm^{-1})
XBL 836-5959

Figure 2

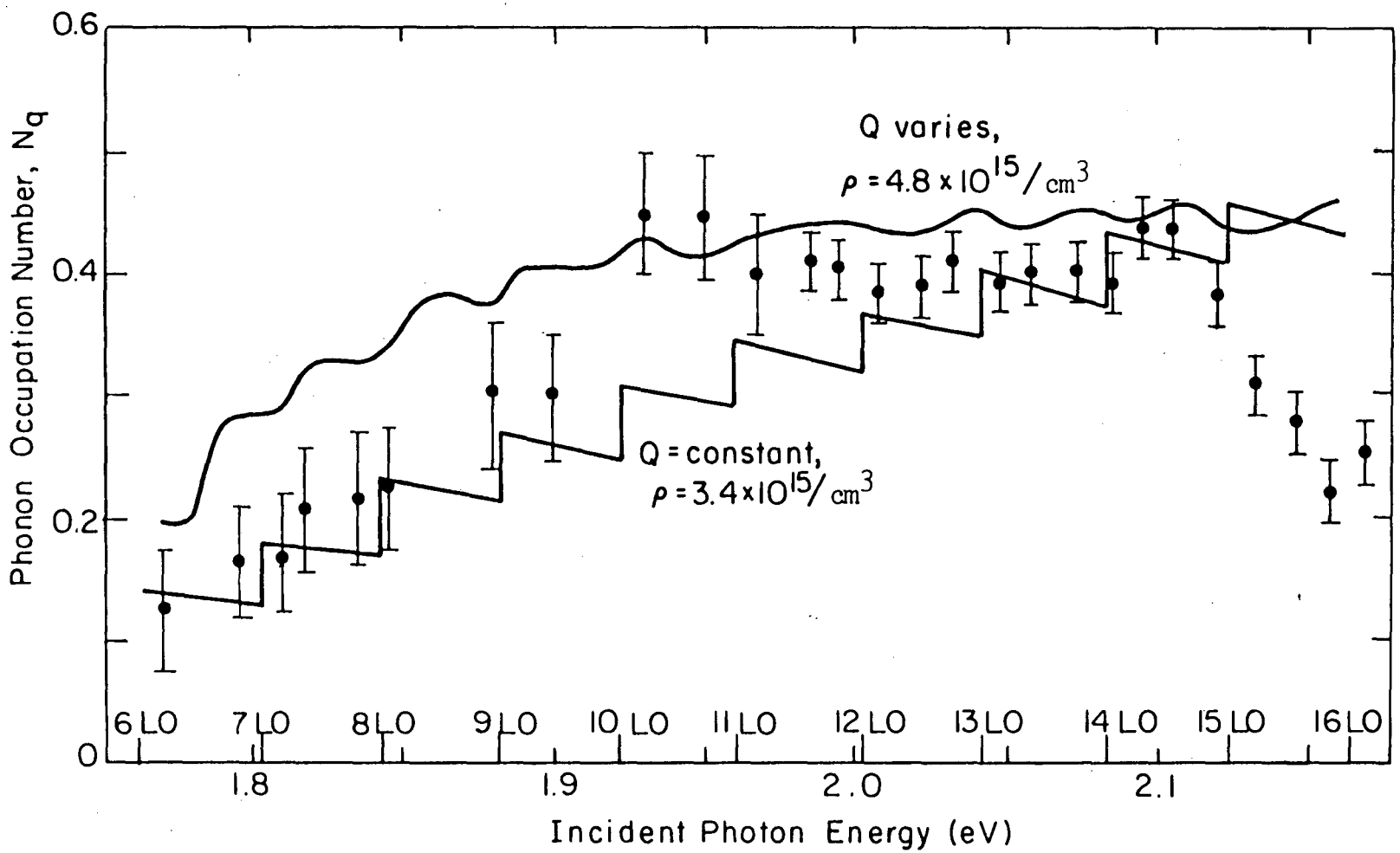

XBL 836-5970

Figure 3

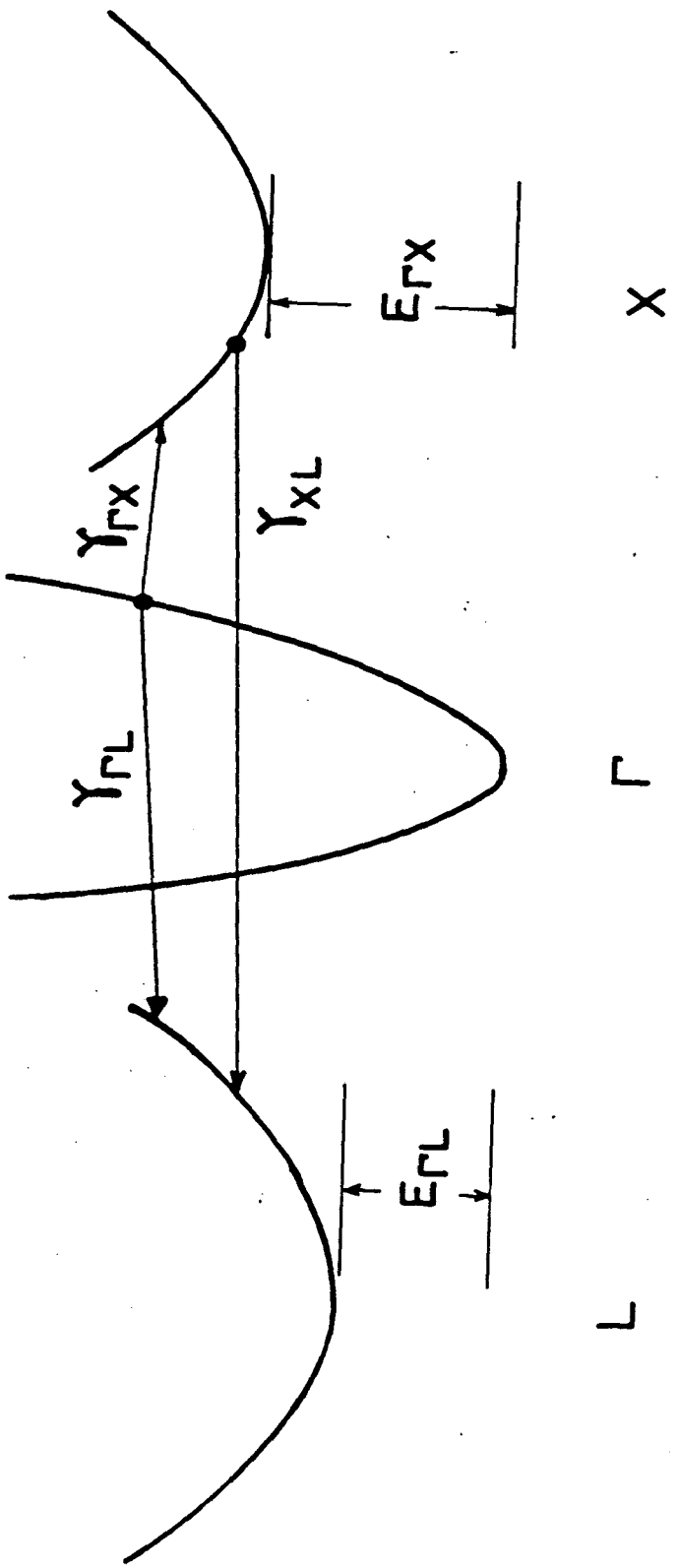
$E_{\Gamma L}$
$\gamma_{\Gamma L}$
$\gamma_{\Gamma X}$
γ_{XL}
$E_{\Gamma X}$
L
Γ
X

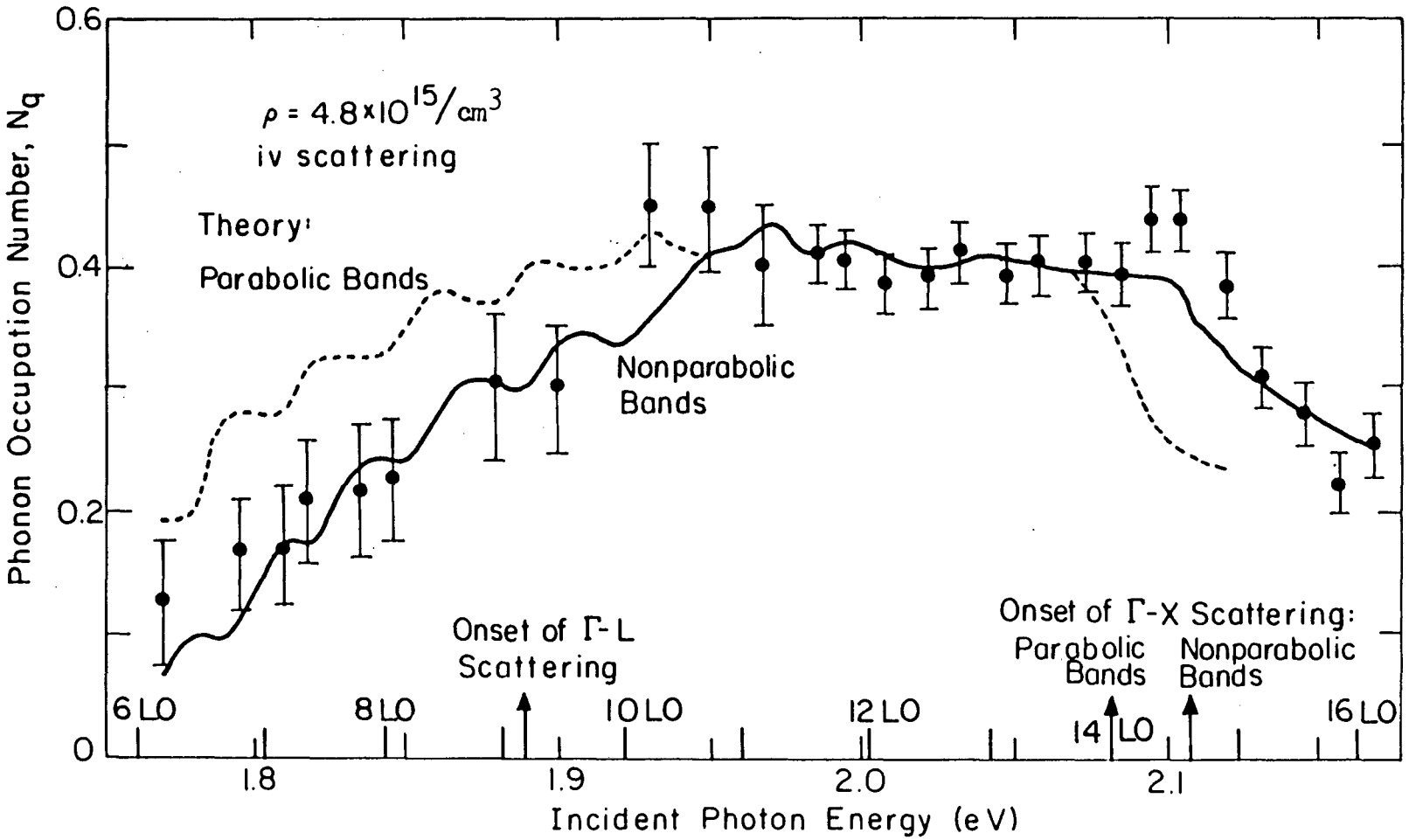

XBL 836-5971

Figure 5

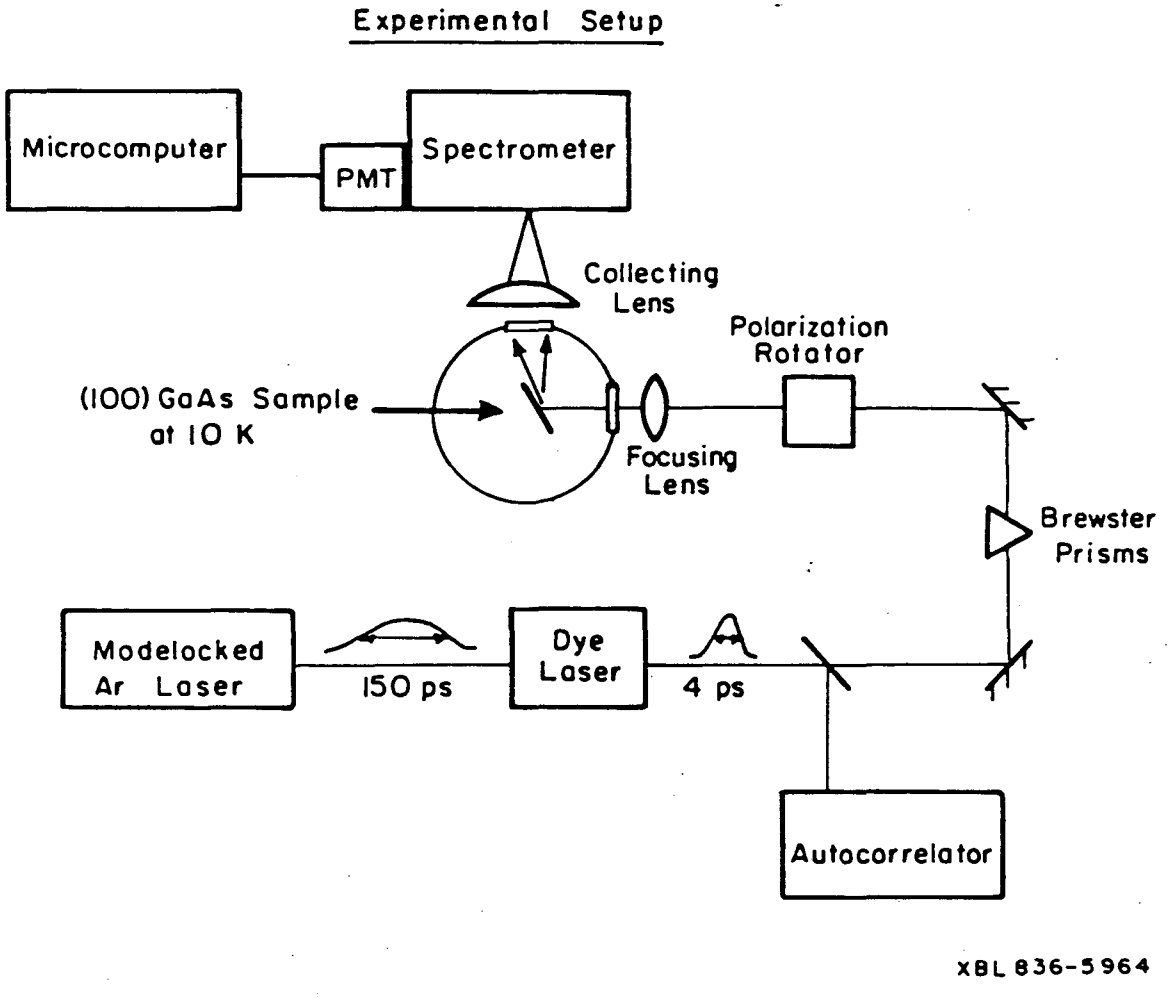
Experimental Setup
Microcomputer
PMT
Spectrometer
Collecting Lens
Polarization Rotator
(100) GaAs Sample at 10 K
Focusing Lens
Brewster Prisms
Modelocked Ar Laser
150 ps
Dye Laser
4 ps
Autocorrelator
XBL 836-5964

Figure 6

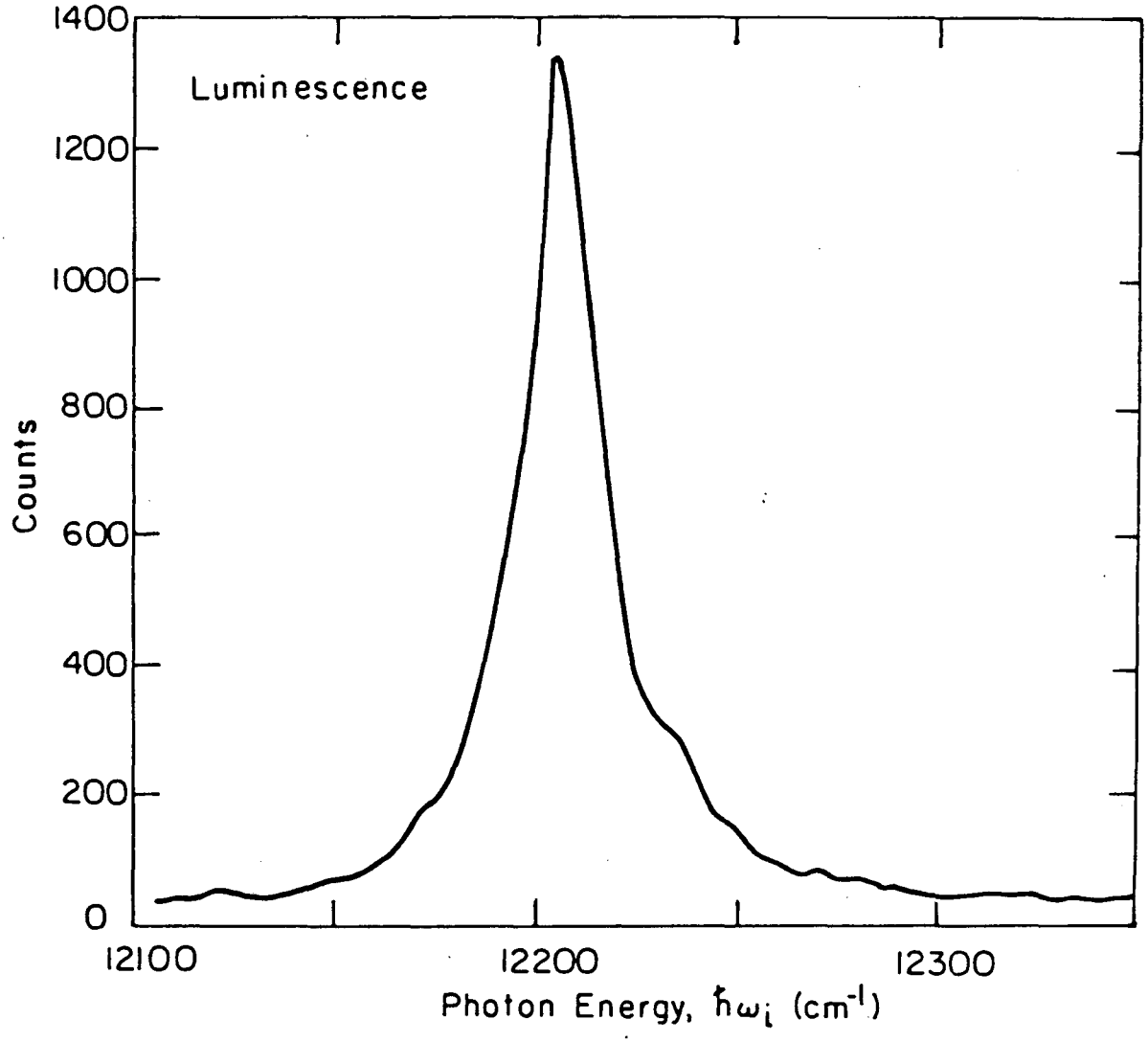

XBL836-5968

Figure 7

Fig. 7

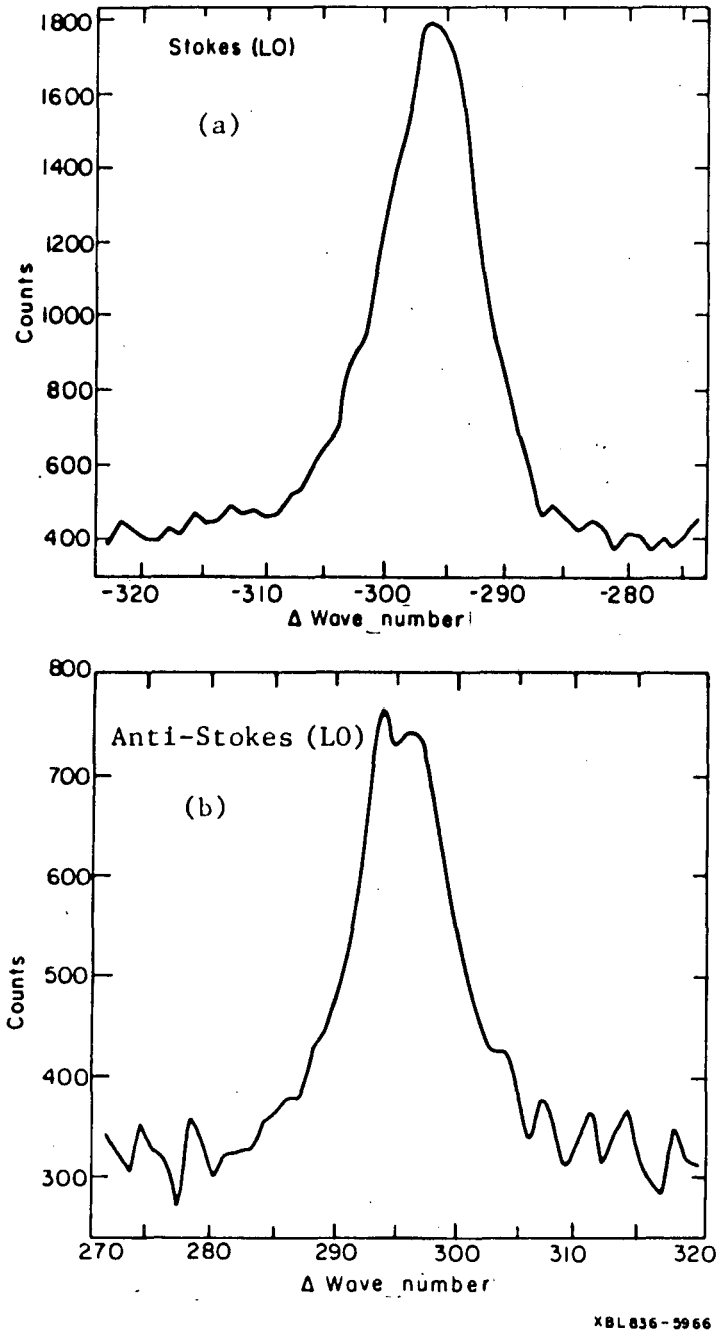
Stokes (LO)
(a)
Counts
Δ Wave number
Anti-Stokes (LO)
(b)
Counts
Δ Wave number
XBL 836-5966

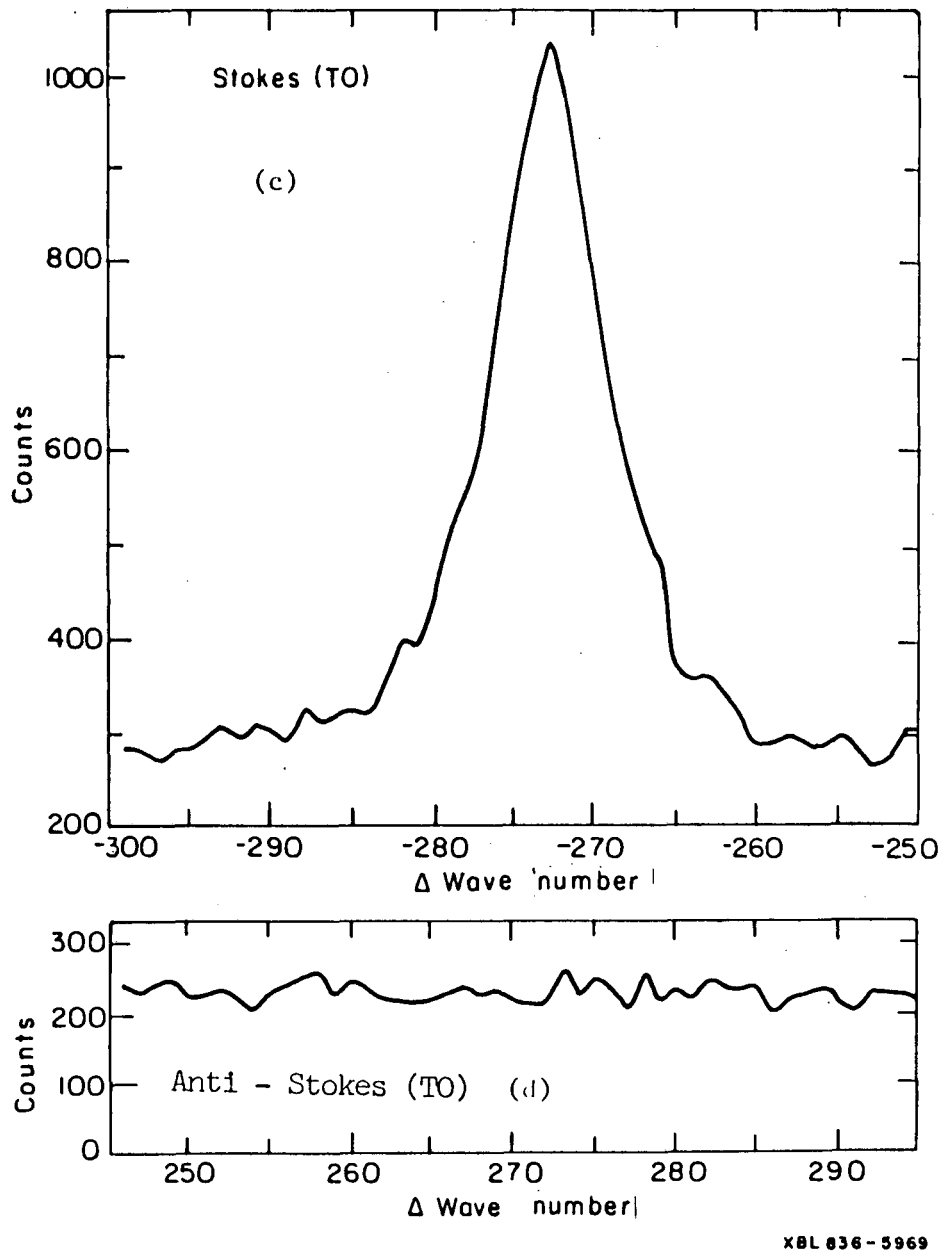
Stokes (TO)
(c)
Counts
Δ Wave number
Anti - Stokes (TO) (d)
Counts
Δ Wave number
XBL 836-5969

Figure 8

This report was done with support from the Department of Energy. Any conclusions or opinions expressed in this report represent solely those of the author(s) and not necessarily those of The Regents of the University of California, the Lawrence Berkeley Laboratory or the Department of Energy.

Reference to a company or product name does not imply approval or recommendation of the product by the University of California or the U.S. Department of Energy to the exclusion of others that may be suitable.

TECHNICAL INFORMATION DEPARTMENT
LAWRENCE BERKELEY LABORATORY
UNIVERSITY OF CALIFORNIA
BERKELEY, CALIFORNIA 94720